Land Cover/Use Classification Using Optical and Quad Polarization Radar Imagery

A thesis submitted in partial fulfillment of the requirements for the degree of Master of Science at George Mason University

By

Arjun Sheoran
Bachelor of Science
Shippensburg University of Pennsylvania, 2005

Director: Dr. Barry N. Haack
Department of Geography and GeoInformation Science

Spring Semester 2009
George Mason University
Fairfax, VA

ACKNOWLEDGEMENTS

I consider myself extremely lucky and fortunate to have come to George Mason University for my MS. I am grateful to my adviser Dr. Barry Haack, who has mentored me throughout and helped me decided on a path of study which I'm passionate about. It is thanks to his support and encouragement that I have been able to transfer my research interests into a thesis and career. Additionally, I am also grateful to my committee members, Dr. Allan Falconer and Dr. Edmund Zolnik for their constant support of my thesis work.

My thesis comes at a time when I was transition from the academic environment into the workforce. This transition would not have been possible without the continued support and guidance of my sister (Nayantara (Tara) Sheoran), friends, and faculty at George Mason University.

I would also like to thank the Alaskan Space Facility under sponsorship from NASA which provided the PALSAR imagery used in my thesis.

TABLE OF CONTENTS

LIST OF TABLES

LIST OF FIGURES

ABSTRACT

LAND COVER/USE CLASSIFICATION USING OPTICAL AND QUAD POLARIZATION RADAR IMAGERY

Arjun Sheoran, M.S.

George Mason University, 2009

Thesis Director: Dr. Barry N. Haack

With the recent increase in the availability of quad polarization (Horizontal-Horizontal, Horizontal-Vertical, Vertical-Horizontal and Vertical-Vertical) radar data, the need to assess the utility of these datasets for land cover/use classification is crucial. Historically, most spaceborne radars were single wavelength and single polarization. For this study, the Japanese ALOS (Advanced Land Observing Satellite) PALSAR (Phased type L-band Synthetic Aperture Radar) quad polarization radar data were obtained at 12.5 meter spatial resolution. The second dataset to be used in this study was acquired by Landsat TM (Thematic Mapper) at a 28.5 meter spatial resolution.

The purpose of this study is to evaluate the classification of various land covers/uses using spaceborne quad polarization radar and optical TM data. Secondly, the study analyzes the utility and improvements that can be made to the radar and TM data with the help of using radar texture and multi sensor fusion techniques, e.g., layer stacking and Principal Component Analysis (PCA).

Three study sites Bangladesh, California and Kenya were chosen for analysis in this study. The primary methodology was spectral signature extraction and Transformed Divergence (TD) separability measures to evaluate the relative utility of the various data types. In addition four texture measures, kurtosis, mean euclidean distance, skewness, and variance and four window sizes were analyzed. Supervised signature extraction and classification (maximum likelihood) was used to classify different land covers/uses followed by an accuracy assessment.

The combination of radar and Landsat consistently provided excellent classification accuracies, well over 90%. Comparing the two datasets Landsat provided higher classification accuracies as compared to radar and radar texture analyzed individually. Variance texture was consistently the best among all four texture measures, as it showed the most improvement in the TD values. The use of texture on radar was helpful when evaluating the separability among the different land covers/uses. However, texture was not able to provide higher classification accuracies for the different land covers/uses as compared to the original radar and Landsat datasets.

1. Introduction

Assessing problems within environmental studies, economic planning, resource management, restoration projects and disaster preparedness requires a scientific analysis of data and using processes available within the geospatial industry. With the launch of new spaceborne radar systems, including RADSARSAT-2 and TerraSAR-X, the application and use of quad polarization radar data within the geospatial industry may prove beneficial. However, the full potential of quad polarization radar data for land cover/use classification and other applications remains in its nascent stages as a result of limited availability and analysis. Only with a detailed understanding of this relatively new operational spaceborne quad polarization data can the scientific and application community maximize the benefits of these technological innovations. To better analyze the utility of quad polarization radar it is imperative that the new data being collected is examined scientifically.

Traditional means of providing reliable land cover/use information is primarily undertaken by multispectral systems such as Landsat Thematic Mapper (TM). These systems, because of their limited functionality in cloud covered areas, are not able to fully sustain the demands for providing land cover/use information for many areas around the world. However, with the success of RADARSAT-1 and other operational spaceborne radar systems, this limitation has been addressed to a certain extent. With the recent success

of operational spaceborne radar systems, a geospatial framework has been established, which provides accurate and continuous data for applications ranging from offshore oil drilling in the Gulf of Mexico to homeland security.

Radar systems (microwave) have distinct advantages over traditional multispectral sensor (visible and infrared) systems which has made the application of radar data indispensable to the geospatial industry. The longer wavelengths of radar are capable of penetrating atmospheric conditions that limit traditional spaceborne optical and multispectral systems (Henderson et al. 2002). As seen in Figure 1, microwaves are longer than all other wavelengths with the exception of radio waves. These microwave wavelengths hold enormous data collecting potential for many geographic areas around the world that are often obscured by cloud cover. Radar is an active sensor, which illuminates the surface with its own energy as opposed to being dependent on daylight as is the case with optical sensors. Radar sensors are capable of precisely measuring the amount of returned energy, i.e., backscatter, and can accurately delineate the terrain regardless of the time and weather (Campbell, 2002).

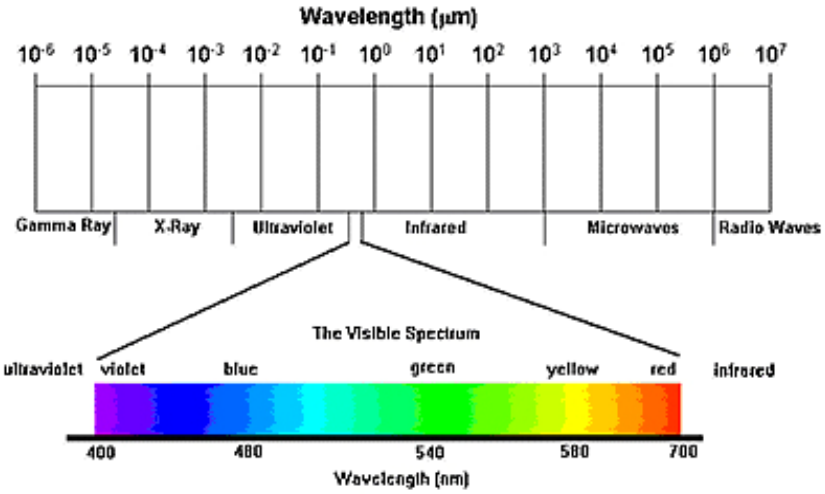

Figure 1: The Electromagnetic Spectrum (EMS). (CRISP, 2001)

All objects emit and reflect electromagnetic radiation. Remote sensing can detect feature characteristics based on the reflectance, absorption and scattering of electromagnetic radiation. Every surface feature has a distinct way in which it interacts with electromagnetic radiation providing unique information. Radar and optical sensors are capable of remotely sensing these interactions and, in turn, are able to provide a better understanding of ground features. These sensors collect spectral information which is commonly referred to as digital numbers (DN). Single surface feature exhibits a variable response across the EMS that is unique, and is generally referred to as the reflectance curve or the spectral signature (Campbell, 2002). All ground features reflect energy in a particular way and similar features exhibit the same reflectance properties. For example healthy green vegetation in the infrared bands will have high reflectance; water is expected to have low reflectance in the infrared bands. Gaining a better understanding of

how certain features interact with electromagnetic energy can help provide unique and validating information.

The surface interaction of radar is very different than optical sensors thus providing unique information about ground features. The response of radar is a function of surface roughness, geometry and internal structure as opposed to surface reflection with optical wavelengths. The variation in radar backscatter from a feature may be a result of incident angle, acquisition date, look direction, moisture on the surface or the physical composition of the feature itself. Backscatter is also strongly influenced by the orientation of the feature to the incoming radar signal. This is particularly true for cultural features such as slanting roof tops. In Asian countries such as Bangladesh, houses are usually roofed with galvanized and corrugated steel sheets commonly referred to as tin. With a slight shift in the incident angle these slanting roof tops can drastically influence the intensity of the return signal resulting in high or low backscatter. Multispectral sensors have often not been beneficial in such settings.

One of the difficulties with the analysis of radar data is that most recent radar spaceborne systems only collect data using a single wavelength with a fixed polarization. Hence only one component of the total surface scattering is being measured, while any additional information contained within the returned radar signal is lost (Toyra et al. 2001; Dell'Acqua et al. 2003). More recent systems, such as the Japanese PALSAR and the Canadian RADARSAT-2, include an increased number of polarizations. Imagery acquired under different polarizations will obtain different backscatter responses and

different informational content (Banner and Ahern, 1995; Hegarat-Mascle et al. 1997; Gauthier et al. 1998).

Like polarizations transmit and receive the same polarizations, i.e., either HH or VV. However, cross polarization, HV and VH are capable of transmitting and receiving polarizations which are orthogonal to each other (Campbell, 2002). Cross polarization, due to its interchangeability is able to provide unique information about surface features which might be lost when using like polarization.

Generally, the visible and infrared wavelength systems are recognized as being superior to radar data, due to their multispectral information content (Brisco and Brown, 1999). This is a strong argument for the utility of sensor fusion. Such multispectral systems are a fusion of several individual bandwidths of information. However, one problem with these systems is that spectral responses in the optical and infrared wavelengths are sensitive to differential scattering and absorption caused by chlorophyll, green leaf areas, and leaf structure leaving some vegetation types that cannot be separated due to the similarity of their spectral responses (Raghayswamy et al. 1996). Radar responds differently to varied terrain and dielectric factors such as plant canopy roughness and structure, plant moisture content and sub-canopy conditions. As such, a combined sensor analysis could contribute to information regarding both the leaf composition and the surface geometry thereby greatly increasing the potential information content (Henderson et al. 2002).

Research objective

The primary objective of this study is to empirically examine the potential of independently using quad polarization radar and optical data to do land cover/use classification. The study also evaluates improvements that can be made to the original datasets (radar and Landsat) to increase the overall classification accuracy by fusing multiple datasets together.

The effectiveness of applying different texture measures to the radar imagery is also addressed. The intent is to determine whether radar texture yields better classification and separability for the various land covers/uses as compared to using original radar. It is also important to determine which texture measures and window sizes provide the best classification and separability results. This question will be addressed using a technique called Transformed Divergence (TD).

The final assessment in this study focuses on determining the best procedure for combining multiple datasets. Layer stacking and PCA are the two procedures used to evaluate the effectiveness of fusing datasets. Layer stacking has been a commonly used technique in the field of remote sensing, where as the use of PCA for classification has been used sparingly. The loss of key spectral information in an image has resulted in PCA not being widely used for land cover/use classification. The intent of this study is uncover some of the flaws in both techniques and determine which process results in minimal loss of key spectral information and in turn providing better classification. Three areas were chosen for this study. Having three study areas eliminates any inconsistencies in the results and also helps to empirically verify the results from one area to another.

2. Methodology and Literature Review

These sections outline the methodologies used in this study, and are arranged in the order in which the analysis and assessments were undertaken. The methodology for all study sites is the same and follows the pattern described below.

2.1 Pre-processing of Data (Radar and Landsat)

The three radar datasets used in this study were acquired from Japanese ALOS and the PALSAR sensor at 12.5 meter spatial resolution. Each radar image covers an area of approximately 65 kilometers x 35 kilometers. The original PALSAR data were in a raw format and had to be georeferenced before it could be analyzed.

A software package (Map Ready 1.0.3) provided by the Alaska Satellite Facility (ASF), was used to convert the raw radar data into georeferenced files. The free software was downloaded from the ASF website. The radar data were converted from the raw format to four 32-bit floating point GeoTiff files (one for each band – HH, HV, VH, and VV). The next step in pre-processing was to convert the GeoTiff files to image (.img) files. It is important to convert the .tiff files to .img files as it allows for a more detailed analysis of the data. The conversion to image files was done using the import module in ERDAS Imagine 9.2. All of the analysis undertaken in this study was done using ERDAS Imagine 9.2.

To process the radar imagery effectively and efficiently, the four image files were converted from 32-bit floating point to unsigned 8 bit. Considering ERDAS Imagine is only capable of displaying an 8-bit image, i.e., on a scale of 0 to 255, it was advantageous to use 8-bit imagery. All PALSAR images were accurately georeferenced at 12.5 meter spatial resolution.

Landsat imagery for the three study areas was acquired from the United States Geological Survey (USGS), via the United States Department of Foreign Agricultural Service. The multispectral Landsat (TM) images had a spatial resolution of 28.5 meter for the three visible (blue, green, red) and three infrared (near infrared, mid infrared, mid infrared) bands. The Landsat images have a foot print (area on ground for one image) of approximately 183 kilometers by 170 kilometers. Access to the USGS imagery archive was a valuable resource throughout the course of this study.

Based on the location of the PALSAR imagery, the Landsat images were obtained for the three study sites. With the exception of one study site, the Landsat images for the other two sites had to be mosaiced together to cover the extent of the radar images. Even though the Landsat images cover a larger geographic area, they were at the bottom of the radar image and hence had to be mosaiced. The Landsat images for Bangladesh and California were mosaiced together using imagery from the same day. Mosaicing of the images was a first step prior to subsetting and resampling the images. The reason for doing so was to protect the overall radiometric accuracy of the datasets.

The next step was to register and resample the Landsat images. The Landsat images were resampled to 12.5 meter using a nearest-neighbor procedure. This was done

to maintain consistency across all images and to avoid any discrepancies during the process. To maintain the texture values of the data, the resampling should be to the smallest pixel of the original data types. During the resampling process all six bands three optical and three infrared bands, were included. As part of this study, the TM panchromatic and the thermal band were not included. The Landsat images were georeferenced to the Universal Transverse Mercator (UTM) coordinate system.

The next step was to rescale all of the Landsat images to an unsigned 8 bit (0 to 255) radiometric resolution. This was done in order to maintain consistency across both datasets (Landsat and radar). The last step was to subset the Landsat images based on the location and size of the radar image. The intent was not only to reduce the overall file size of the Landsat image, but also to avoid any unnecessary classification of pixels.

2.2 Transformed Divergence (TD)

Transformed Divergence, which is calculated from the means and covariance matrices of each spectral class or calibration site, is a measure of the statistical distance between class or site pairs of interest and provides information on their separability. This separability is an indirect estimate of the likelihood of correct classification between different datasets or derived measures (Swain and Davis, 1978). Such an estimate provides information usually obtained by the time consuming and expensive process of actual classification and accuracy evaluations. A TD value of 1,500 or greater generally indicates an acceptable separability of classes (Latty and Hoffer, 1980). The TD separability level does vary as a function of the complexity of the input data. It is lower

for simpler datasets and higher for more complex data. The maximum or saturated TD value is 2,000.

In previous studies undertaken by Haack (1984), TD was not only used to determine the best number of files/bands for classification purposes, but also for selecting specific datasets. Similarly, in this study, TD is used to select the optimum texture measure along with the best window size, for classification purposes. The reason for using TD as a base for determining the classification datasets is primarily a function of increasing efficiency and reducing redundancy in the actual classification.

Prior to evaluating the TD, spectral signatures were extracted from the areas of interest (AOIs) for each of the three study areas. One AOI was used for each class. These AOIs were identified using ancillary information such as Google Earth and other sources. Spectral signatures were extracted from the four AOIs for each study area and TD values were then calculated to evaluate the separability among the various classes. The use of TD was to determine the relative value of the different data for land cover/use delineation including the use of variance texture as compared to the original radar and TM bands. The separability results or TD values for the different land covers/uses were the foundation for selecting which radar texture measure would be used for classification purposes.

2.3 Texture Measures Radar Imagery

After both sensor datasets were georectified, resampled, and AOIs identified, four texture values were extracted from multiple window sizes (5 x 5, 7 x 7, 11 x 11 and 13 x 13). Previous studies conducted by Idol et al. (2007) and Sheoran et al. (2007) have

suggested little improvement in separability and classification values by using a 9 x 9 window size. Therefore, the 9 x 9 window size has not been evaluated in this study.

In this study, texture was only applied to the PALSAR imagery and not the optical data. Mean eucliden distance, variance, skewness and kurtosis are the texture measures available within ERDAS, and hence all four were chosen for comparison. Texture was calculated on radar imagery for all three study sites. A comparison was made between the TD values for the original radar and radar texture. The first texture measure applied to the radar image was mean euclidean distance (1st order)

$$= \frac{\sum[\sum(x_{c\lambda} - x_{ij\lambda})^2]^{\frac{1}{2}}}{n-1}$$

Where,

$x_{ij\lambda}$ = DN (Digital Number) value for spectral band λ and pixel (i, j) of a multispectral image

$x_{c\lambda}$ = DN value for spectral band λ of a window's center pixel

n = number of pixels in a window

The second texture measure used on the radar images was variance (2nd order),

$$= \frac{\sum(x_{ij} - \overline{X})^2}{n-1} \qquad \overline{X} = \frac{\sum x_{ij}}{n}$$

Where,

x_{ij} = DN value of pixel (i, j)

n = number of pixels in a window

$\overline{X}$ = Mean of the moving window (kernel)

The third order of texture used on the radar images was skewness,

$$= \frac{\left|\sum(x - \overline{X})^3\right|}{(n-1)(\sigma)^{\frac{3}{2}}}$$

Where,

x_{ij} = DN value of pixel (i, j)
n = number of pixels in a window
$\overline{X}$ = Mean of the moving window (kernel)
σ = Variance

The fourth order of texture used on the radar images was kurtosis,

$$= \frac{\sum (x_{ij} - \overline{X})^4}{(n-1)(\sigma)^2}$$

Where,

x_{ij} = DN value of pixel (i, j)
n = number of pixels in a window
$\overline{X}$ = Mean of the moving window (kernel)
σ = Variance

Textural information may be as important as spectral information in radar, as the information content of an image resides in both the intensity (spectral) of individual pixels and the spatial arrangement of the pixels (Anys and He, 1995; Kurosu et al. 1999). Standard image classification procedures used to extract information from remotely sensed images usually ignore this spatial information and are based on purely spectral characteristics. Such classifiers may be ineffective when applied to land classes such as residential and urban areas that are largely distinguished by their spatial rather than their spectral characteristics (Solberg and Anil, 1997; Townsend, 2002). The advantages of using derived radar measures, such as texture measures at different window sizes, in comparison to original radar data, has been demonstrated by Haack et al. (2002) and Herold et al. (2005).Textural information may be used in combination with the spectral measurements of a wavelength for analysis (Nyoungui et al. 2002; Huang et al. 2007). Texture is particularly useful for features in the natural environmental, because it reflects

the local variability of grey level in the spatial domain revealing unique information about the ground features (Zhang et al. 2008).

2.4 Fusing of Data

Over the years the fusing of data from multiple sensors has been a common technique and this trend is bound to continue as the geospatial technologies improve. With its origin in military application, image fusion has provided a framework for the civilian sector which helps integrate different sensor platforms for a variety of uses (Roberts et al. 2008). According to Chavez et al. (1991), one of the reasons for this increase in fusing multiple datasets is due to the complimentary information of the different datasets. It is crucial for the scientific community to harness this potentially useful technique as it will immensely improve the geographic knowledge of remote regions across the world. Fusing data from multiple sensors, i.e., Landsat and radar, has proved to be an exceptionally efficient technique in reducing the overall ambiguity in the datasets. Previous studies conducted by Huang et al. (2007) and Sheoran et al. (2007), have suggested an increase in the overall classification values by fusing multiple datasets together.

The availability of remotely sensed data for the same geographic area obtained from separate sensors operating in different portions of the electromagnetic spectrum, such as Landsat TM and PALSAR, has increased greatly. This, along with improved technology for the processing and fusing of such separate datasets, has made the synergies between optical and radar data for land applications of greater practical importance (Leckie, 1990; Pal et al. 2007). The fusing of data from different sensors is

done in an attempt to generate an interpretation of a geographic area that is not obtainable from any single sensor alone. This is also done to reduce the uncertainty associated with data from a single source (Schistad et al. 1994; Saraf, 1999; Simone et al. 2002). Image fusion over the years has become a useful technique in the remote sensing field, not only making the interpretation process faster and more reliable, but also providing unique and accurate information for the extracted features (Wen and Chen, 2004). There are distinct advantages of fusing radar with optical data, as the end product has the advantage of textural information (radar image), and spectral information from the optical and infrared bands. Hence, by fusing multiple datasets, an analyst has a single and more informative image (Pal et al. 2007).

In this study there are two procedures for fusing the different datasets together, PCA and layer stacking. Principal Component Analysis in the field of remote sensing is used quite sparingly due to the occasional loss of key spectral information in an image, where as layer stacking is commonly used to combine different datasets. The primary motive in this study is to determine if overall classification accuracies can be improved without loss of key information. A comparison would be made between the accuracy attained using the two techniques, in order to determine which procedure is better suited for land cover/uses classification. The two techniques would be applied to the following datasets:

1) original radar with Landsat;
2) radar texture with Landsat.

Each of these combinations of data were first analyzed using a traditional layer stacking procedure, which was followed by calculating PCA of the Landsat and combining it with the PCA of radar original and radar texture.

Layer stacking is a comparatively straight-forward image processing module as compared to PCA. Layer stacking is a process in which different bands are combined with each other to generate a single image with multiple bands. One of the advantages of layer stacking resides not only in its simplistic nature, but also in its efficiency and geometric accuracy to combine bands from different sensors. Secondly, layer stacking does not restrict the number of bands which can be evaluated at one time. This provides an option of stacking a large number of bands from different datasets together and evaluating separability or classification accuracy.

In a previous study by Idol et al. (2007), layer stacking was the primary method for combining different bands and datasets. In their analysis, layer stacking provided the platform for yielding good classification and separability results. Similarly, in a preliminary analysis conducted by Sheoran et at. (2007), layer stacking was also successfully used to combine different bands and datasets together.

Principal Component Analysis is the second technique used in this study for fusing datasets. One of the advantages of using PCA is its efficiency to summarize the most dominant spatial and spectral characteristic of the datasets (Henebry and Rieck, 1996). This ability to extract the most valuable component within the imagery is one of the reasons for selecting PCA as part of this study. Secondly, PCA also helps in reducing the overall redundancy in the dataset by combining the Landsat and radar data bands to

create a single image which is more interpretable. PCA is able to extract the most dominant spectral characteristic by means of data compression, i.e., large amounts of information is compacted into fewer bands by reducing the dimensionality of the data (Jensen, 1986).

Principal Component Analysis in this study is used to evaluate its effectiveness as a classification technique by combining the spectral information from Landsat and the textural content of radar imagery. PCA has been successfully used in previous studies for land cover mapping and geological assessments (Pal et al, 2006; Chavez et al, 1991). However, this study will evaluate its effectiveness for land cover/use classification, ideally with little loss in spectral information.

In a recent study conducted by Nikolakopoulos (2008), PCA was evaluated in combination with eight other fusing techniques, and all techniques including PCA were found to improve the spectral resolution and the visual result. However, the effectiveness of using PCA as a fusing technique for classification depends on the datasets being evaluated and also on the analysts experience with using the technique. Even though the use of PCA might result in good quality images, one of the limitations of this technique, as reported in many research papers is the concern over color distortion and loss of spectral information (Nikolakopoulos, 2008).

Similar to the methodology for layer stacking, PCA will be used on the original radar, radar texture, and Landsat imagery. Only one component from each of the datasets would be extracted and fused with the other dataset. For example, one principal component from the original radar (four bands) will be combined with the one

component of Landsat (six bands). Similarly, one component of Landsat will be combined with one component of radar texture (four bands). Originally, it was presumed that taking three principal components from each datasets would be better. However this was not the case as some of the land covers/uses for two of the three study sites were not successfully classified. Taking a larger number of principal components has been known to erode some of the finer spatial detail in an image (Henebry and Rieck, 1996) and this is one of the reasons the study only evaluates one component from each dataset, i.e., radar and Landsat. In a previous study, Chavez et al. (1991) successfully evaluated the spectral characteristics of multiple datasets based on one principal component.

2.5 Classification

The final step in the analysis was to classify the images. The process of classification in essence is segmenting the images into unique classes or informational categories based on land covers/uses. In this study, signature extraction was used and a maximum likelihood decision rule was applied. It is essential to choose a decision rule which would effectively determine the likelihood of membership to each of the two, or more classes. The algorithm for maximum likelihood decision rule is based on means and variances of the different training spectral signatures. It analyzes each pixel individually and compares it to the signatures extracted via the decision rule algorithm. Due to the nature of the decision rule each pixel is assigned to only one of the classes. In essence this algorithm evaluates and assigns a pixel within an area of overlap to a class which it is most likely a member off, based on its spectral signature value. The likelihood of a pixel being classified to the right class increases the probability of a correct classification

(Herold, 2000). Within each study site the maximum likelihood classifier was applied to a number of different datasets including the following:

1. original radar;
2. radar texture;
3. original radar and radar texture;
4. optical; and
5. fused datasets.

The process of image classification can be divided into two steps. The first step is to define the criteria by which the images would be segmented and recognized, referred to as signature extraction. The second step entails evaluating these extracted signatures and assigning image pixels to classify the entire image using a statistical decision rule of maximum likelihood.

The process of signature extraction is based upon the analyst's knowledge of a particular study area. Particularly in the case of supervised signature extraction, it is essential to have a good understanding of the land covers/uses present on the ground to identify particular AOIs for extracting signatures. For this study, four different land covers/uses were identified for each of the three study sites.

The AOIs from which the signatures are extracted are commonly referred to as training sites. Selection of the training sites is one of the most important aspects of the classification process. Ideally a training site would be homogeneous and would be representative of the overall land covers/uses. Selecting training sites for the three study sites was based on ancillary information from Google Earth and USGS Landsat images. It

is important not to misidentify a land cover/use in a training site because this will lead to misclassification during accuracy assessments.

The second step in the classification process is where all the image pixels are classified based on the training sites. The classification of image pixels is based upon the statistics, DN values of the training sites/spectral signatures, associated with each of the different land covers/uses. Based on the statistical values from the training sites, all image pixels are classified to a particular category, e.g., forest, water, residential or almond plantations. For example the decision as to whether or not a pixel is classified as a particular land cover/use, is dependent upon a particular decision rule set by the user (Herold, 2000). In this study the maximum likelihood decision rule was used across all three study areas. Once an entire image has been classified into different categories, based on the spectral signature extracted from the training sites, the next step is to evaluate accuracy.

2.6 Accuracy Assessment

The process of determining accuracy for a classified image is one of the most important steps undertaken in post classification. A classified image for land cover/uses without an accuracy assessment is not considered reliable as it does not convey any scientific consistency.

To undertake an accuracy assessment it is essential to have ground truth or validation information. Validation sites identified in this study are polygons and not individual pixels. The decision to use polygons over pixels for validation purposes in most cases influences the accuracy results (Haack, 2007). Generally polygons tend to

provide relatively lower accuracies, as compared to taking individual pixels. However, when texture is applied to radar imagery, polygons tend to be better validation sites (Herold et al.2005). Considering texture is used in this study, polygons would serve as better validation sites as opposed to individual pixels.

These validation sites represent the known location for particular land covers/uses which are then used to evaluate the classified image. The accuracy of a classified image can be determined by comparing the classified image to the validation sites. Ideally, there should be multiple validation sites for each land cover/use to reduce any discrepancies during the accuracy assessment. For the purpose of this study, two validation sites were used for each of the four classes. Validation sites for Kenya and Bangladesh were based on ancillary information and also visual interpretation of the known land covers/uses. The validation sites for California were based on a 2007 USDA land cover thematic map. When selecting the validation sites it was particularly important to avoid any mixed pixels (pixels containing two or more land covers/uses), as they reduce the overall reliability of the accuracy assessment.

It was also crucial to avoid using the training or calibration pixels for validation purposes. Hence, different AOIs were created for validation purposes for all three sites. One of the reasons for selecting different AOIs for validation is to ensure there is no bias in the accuracy assessment, i.e., the validation pixels do not have a relationship to the pixels in the training AOI used for classification. Classification accuracies can be summarized in an error matrix or a contingency table. An example of a contingency table is in Table 1.

Table 1: Example of a contingency table for accuracy assessment.

Example for radar data					**Users Accuracy**
Land covers/uses	Water	Residential	Agriculture	Forest	
Water	**16264**	4	1326	706	**88.9**
Residential	0	**4655**	1073	109	**79.7**
Agriculture	2	1852	**1324**	620	**34.9**
Forest	9	236	1438	**914**	**35.2**
Producers Accuracy					
	99.9	**69.0**	**25.7**	**38.9**	
Overall Accuracy					**75.8**

Each of the four land covers/uses are identified in the top columns and correspond to the same classes in the rows. The four classes have a number of correctly classified pixels, which are represented diagonally, e.g., 16,264 for water, 4,655 for residential. The number of pixels for each class in the nondiagonal column represents the misclassified pixels. Misclassified pixels in the columns are referred to as errors of omission, i.e., classification has occurred by omitting true area from the classified image. On the other hand, the misclassification in the rows is referred to as the error of commission, i.e., pixels have been wrongly classified and have been placed in their current class (Herold, 2000).

In the case of water, both of these types of errors are present. Nine pixels have been omitted from being classified as water, and have been classified as forest. This misclassification corresponds to both the users error of commission and the producers error of omission. Both of the errors are interrelated, as every error is basically an omission from the correct class and a commission to the incorrect class. Another example of misclassification is to look at the pixel values for agriculture, where the majority of the

pixels have been misidentified as forest (1,438) and water (1,326), resulting in low producers and users accuracy. Overall agriculture has a high error of omission and a low error of commission, resulting in high users and low producers accuracy.

The overall classification accuracy is quite often used for comparison purposes; however, it alone is not reflective of the users and producers accuracy. It is quite common to find a high overall accuracy and low producers accuracy for certain classes as seen in Table 1. The overall accuracy is at 76%, however, the users and producers accuracy for forest and agriculture are exceptionally low. Hence, for analysis purposes it is important not only to evaluate the overall classification accuracy, but also the users and producer accuracy.

Overall classification accuracies are calculated by summing all the diagonal values (correctly classified pixels) in the matrix and dividing them by the total number of pixels. Considering there are two different types of error, i.e., error of omission and error of commission, both the users and producers are calculated differently. The producers accuracy is reflective of how well a ground sample is likely to be classified, and is concerned with the errors of omission. The producers accuracy is calculated by dividing the correctly classified pixels for each cover type by the total number of pixels in the columns. On the other hand, the users accuracy is concerned with the error of commission and is calculated by dividing the total number of correctly classified pixels for a particular class by the total number of pixels in the row. The users accuracy is important because it represents the reliability of a map and how well it represents what is

really present on the ground. This information is important for any map users and is referred to as the users accuracy.

It is the combination of all three classification accuracies which help provides a detailed classification accuracy profile. It is important to report all three classification accuracies, as they all are reflective of how well a particular class is being represented.

3. Study Area and Datasets

The three study sites chosen for this study include two international sites and one U.S. site. The sites are in central Bangladesh, the central valley of California, and southern Kenya (Nairobi). PALSAR imagery for all three sites was acquired between March and May of 2007.

All three sites are quite different, and hence this is one of the reasons that the four classes chosen for evaluation purposes are different from each other. Considering the premise of this research is to determine the utility of using quad polarized radar and optical data for land cover/use classification, differences in land cover/use among the three study sites will not be a major impacting factor.

3.1 Bangladesh

This study site is located approximately 35 kilometers northwest of the capital city of Dhaka and 16 kilometers east of the two major rivers of Jamuna and Ganga (Figure 2). The upper left corner of the image is located at 24^{o} 09’ 32” N and

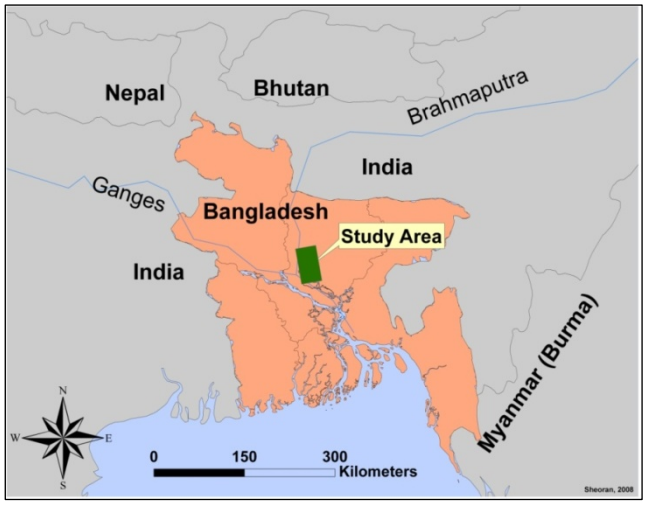

Figure 2: Study site, Bangladesh

89° 48’ 46” E. The bottom right corner of the image is at 23° 38’ 56” N and 90° 16’ 11” E. The PALSAR image (Figure 3) for Bangladesh was acquired on 23rd, March 2007, and the TM imagery (Figure 3) on 14th, March 2003.

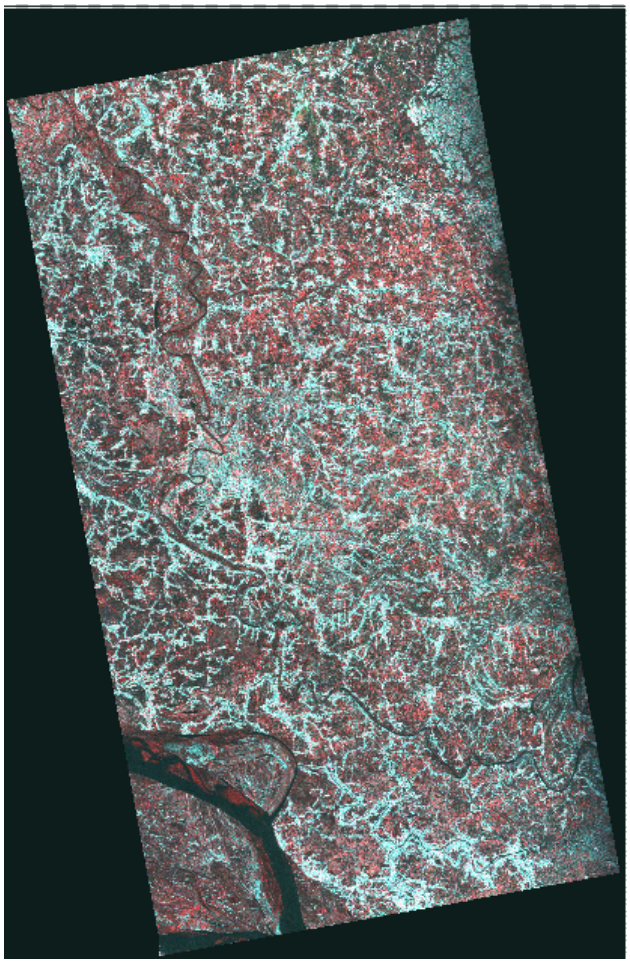

Figure 3: PALSAR image (65 Kilometers by 35 Kilometers) for Bangladesh Acquired 14th, March 2003 (polarization-HH, HV and VH; RGB).

The images for Bangladesh were acquired in different years. However, this would not be much of an impacting factor since both images were acquired in the same season. Secondly, there has not likely been any substantial change in the four land covers/uses. The four classes identified for Bangladesh are water, residential, agriculture and forest.

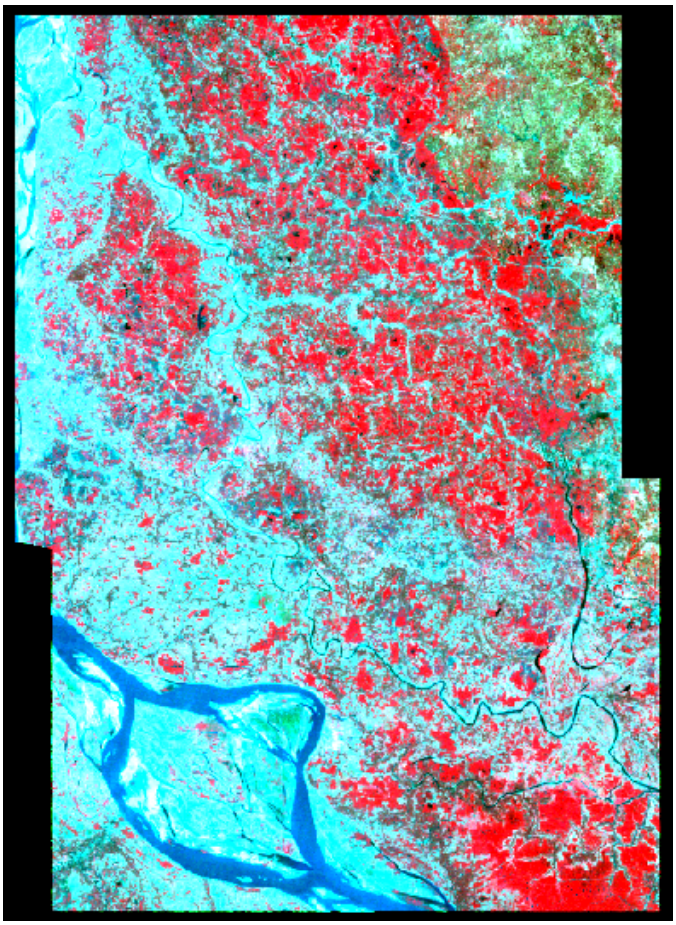

Figure 4: Subsampled Mosaic of TM images (76 Kilometers by 51 Kilometers) for Bangladesh. Acquired 23rd, March 2007 (Bands 4-3-2; RGB).

Bangladesh typically has a monsoon climate, with a mean annual rainfall of 180 centimeters (Islam and Weil, 2000). Primary seasons in Bangladesh include the hot and humid summer from March through June, the hot and rainy monsoon from July to November, and the warm-hot dry winter from December to February.

The majority of the study site is located in low lying areas of the country, with an average elevation of 10 meter above sea level. This region is rich in alluvial soils, making agriculture the primary occupation of the country. During the summer monsoon, land is inundated with water, making rice paddies a common agricultural practice.

The presence of water and moisture in Bangladesh influences the backscatter properties of the radar signal. Moisture content occasionally tends to mute the incoming radar energy, hence providing low backscatter. However, imagery used in this study was acquired in the pre-monsoon season and the presence of moisture was not as much of an impacting factor as it would be during the wet season.

The majority of high backscatter (light turquoise tones) on the radar image is from trees which are in close proximity to small houses. High returns are seen throughout Figure 3 because the study site is primarily agricultural with villages throughout. Almost all farming communities in the area have trees around their agricultural fields, resulting in high backscatter. Additionally, the presence of small houses with tin roofing among the trees strengthens the backscatter.

The agricultural fields are fairly evenly distributed throughout the image and can be seen in light red tones on the radar image. Forested areas comprised of mangroves can be seen in the top right corner of the image. There are also a few clusters of forest in the upper left portion of Figure 3. However, they are not large enough to be used for the purpose of this study. Rivers and other water bodies have a dark tone and are easily detectable in Figure 3. Water can be easily delineated from the surrounding land covers/uses due to its low backscatter. Water acts in a specular manner, i.e., reflecting energy away from the sensor, resulting in low backscatter.

The land covers/uses for agriculture, water and residential are clearly distinguishable on the Landsat image (Figure 4). As seen in the Figure 4, only the blue, green and the near infrared bands have been displayed creating a traditional color infrared

image. Due to sensitive nature of infrared bands to level of chlorophyll in vegetation, the agriculture fields have a vibrant red tone as seen throughout the image. Water can also be clearly delineated with light blue tones, particular on the lower left corner of the image. Residential class appears to have a turquoise tone which makes them visually quite different from the surrounding land cover/uses. Forests in the Landsat image are isolated to the top right corner, and have a green tone.

3.2 California

The second site is located in the central valley of California. The upper left corner of the image is located at 37^{o} 02' 05"N and 120^{o} 50' 15" W. The bottom right corner of the image is at 36^{o} 31' 40" N and 120^{o} 18' 26" W. The study area is approximately 180 kilometers southeast of San Francisco and situated between the Coast Range and the Sierra Nevada Mountains (Figure 5). This part of California is known for its high agricultural productivity particularly for fruit and is commonly referred to as the "Fruit Basket of the World".

Figure 5: Study site, Central valley of California.

The PALSAR imagery (Figure 6) for this study site was acquired on May 1st, 2007 and the Landsat data (Figure 7) was acquired on May 11th, 2007.

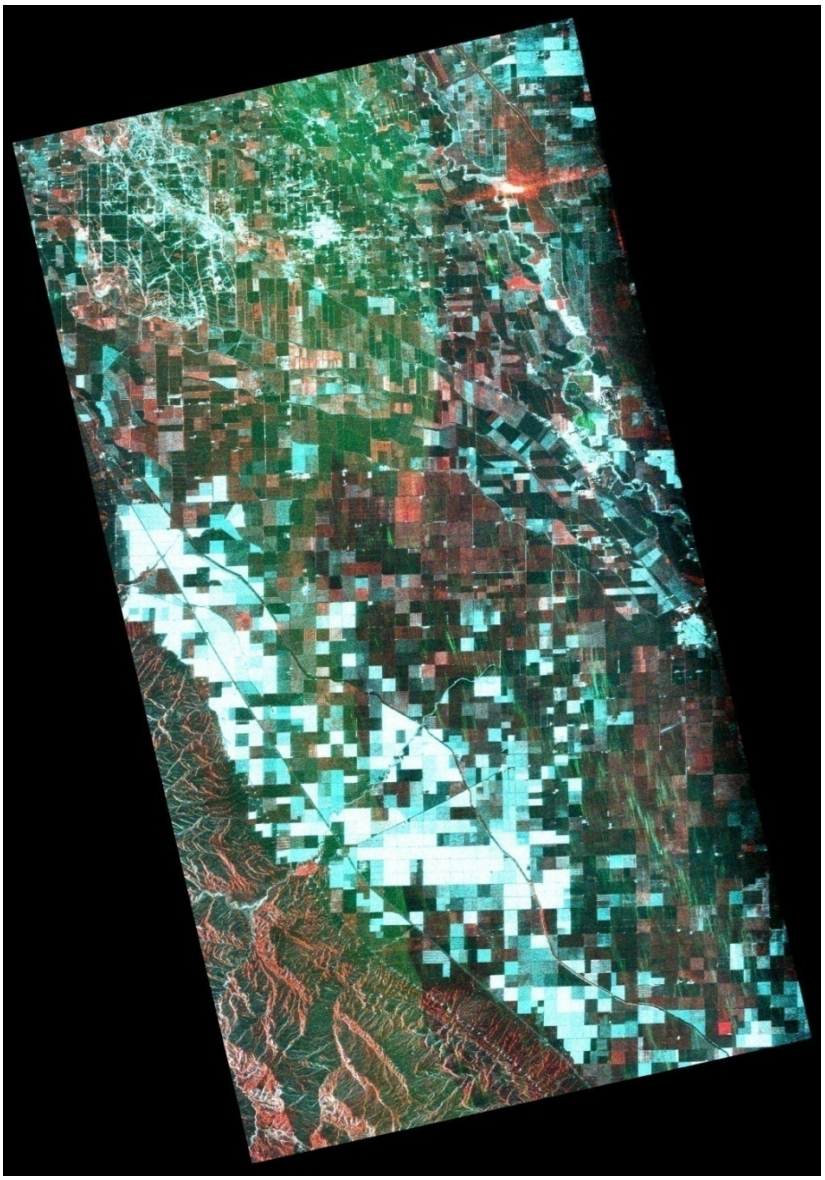

Figure 6: PALSAR image (65 Kilometers by 35Kilometers) for California Acquired 1st, May 2007 (polarizations VV, VH, HV; RGB).

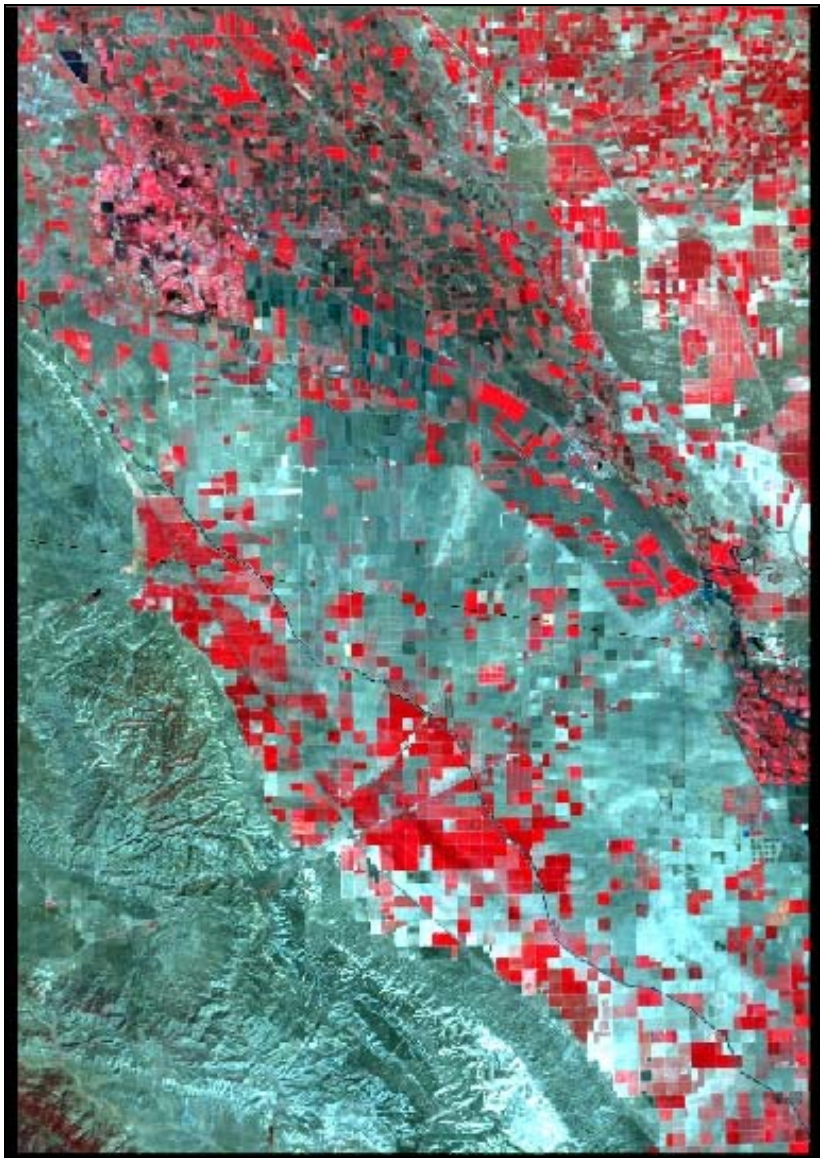

Figure 7: Subsampled Mosaic of TM images (76 Kilometers by 51 Kilometers) for California Acquired 11th, May 2007 (Band 4, 3, 2; RGB).

Unlike the previous study site, it was critical to have the same seasonality in images for California. The reason for having a common seasonality in the two images relates to the types of classes indentified in this section. As opposed to using generic land covers, this study site focuses on distinguishing individual agricultural crops. The four

land covers/uses identified for California included almonds, cotton, fallow/idle cropland and alfalfa. Considering that these areas of interest are quite specific, small changes in seasonality (temperature and moisture) would cause discrepancies during Transform Divergence and classification. Hence, it was essential to use imagery acquired for the same year and at the same time in growing season.

On the radar image one can see a variety of different tones, related to the diversity of various crop types grown in this part of California. Each crop has a unique spectral signature, resulting in the variation of tones. According to the USDA there are well over 100 different types of land covers/uses in this area (USDA, 2007). There is very little residential and urban land cover in this region, as the majority of the flat valley is used for agricultural purposes. This part of California has a typical Mediterranean climate, with hot and dry summers and cool and damp winters.

The imagery for this study site was acquired during late spring when there is very little fallow and bare ground surface. This is due to the intensive agricultural practices in the area. On the radar image, there are a few dark areas, and without ancillary information they could be confused with fallow or bare ground. However, this is not the case, as these dark areas are early-stages of cotton fields. Cotton fields have low radar backscatter due to the crop not being fully matured. A fully matured cotton crop would have higher radar returns. If the same imagery would have been acquired in September the cotton fields would have had a stronger radar signal and thus would have appeared brighter.

Almonds and alfalfa can be clearly distinguished on the Landsat image (Figure 7). Both these classes have a vibrant red tone, which separated them form the surrounding land covers/uses. On the other hand, cotton and fallow visually look very similar to each other with light grey tones in the center of the image. Visually, it is rather hard to delineate these two classes, as they appear to have a blue-gray tone. It is after looking at DN values and ancillary information (field patterns in Google Earth) for these two classes that they were accurately identified.

Using California as one of the study sites is interesting because of the ancillary information known for the site. Detailed 2007 land cover/use classification maps were obtained from the USDA for calibration and validation purposes. Land cover/use maps provided by USDA were based on classification of Landsat and AWiFS imagery. These classified land cover/use maps provided reference information which was used regularly during the analysis of California. A direct comparison was made between the USDA Landsat classified image and the classification accuracies obtained in this study. More importantly for accuracy assessment the classified images were compared to independent validation/truth sites identified on the image itself.

3.3 Kenya

The final study site is Nairobi (Figure 8), Kenya approximately 50 kilometers east of the Rift Valley. The upper left corner of the image is located at 1^{o} 12’ 04” S and 36^{o} 43’ 09” E. The bottom right corner of the image is at 1^{o} 42’ 55” S and 37^{o} 08’ 52” E.

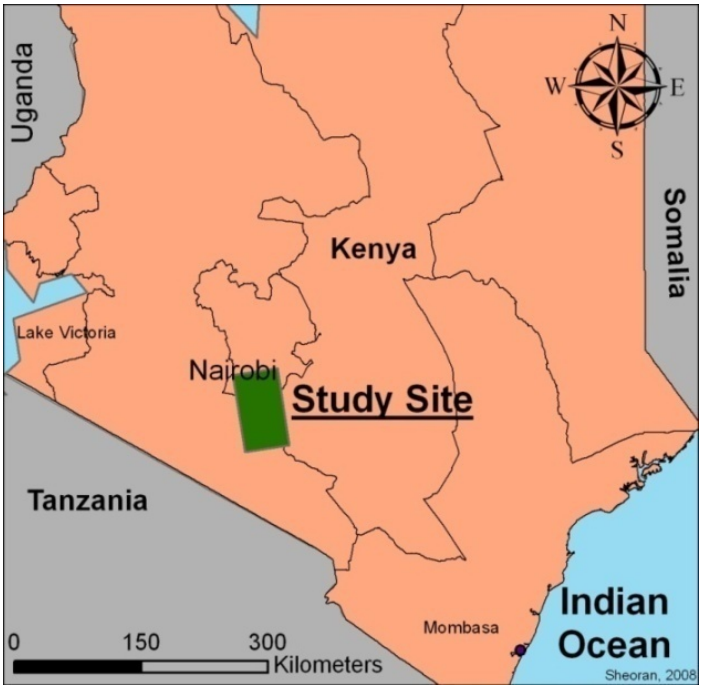

Figure 8: Study site, Nairobi, Kenya.

The PALSAR imagery (Figure 9) was acquired during the rainy season on May12th, 2007. Due to the lack of cloud free optical data for the region, the TM image (Figure 10) was acquired on February 1st, 2000. The TM images were acquired during the hot and dry season. However, this difference in seasonality should not be much of an impacting factor, as most of the land covers/uses identified for this study site are not affected by seasonality. This region of Kenya has a tropical climate with variations in temperatures primarily due to the diverse terrain and altitude.

The four land classes identified for this study site include residential areas, urban areas, savanna and bare ground. The lack of any major water bodies and agricultural fields in the areas resulted in them not being one of the classes. However, the four land

covers/uses provide sufficient variability to successfully evaluate the study site for separability and classification purposes.

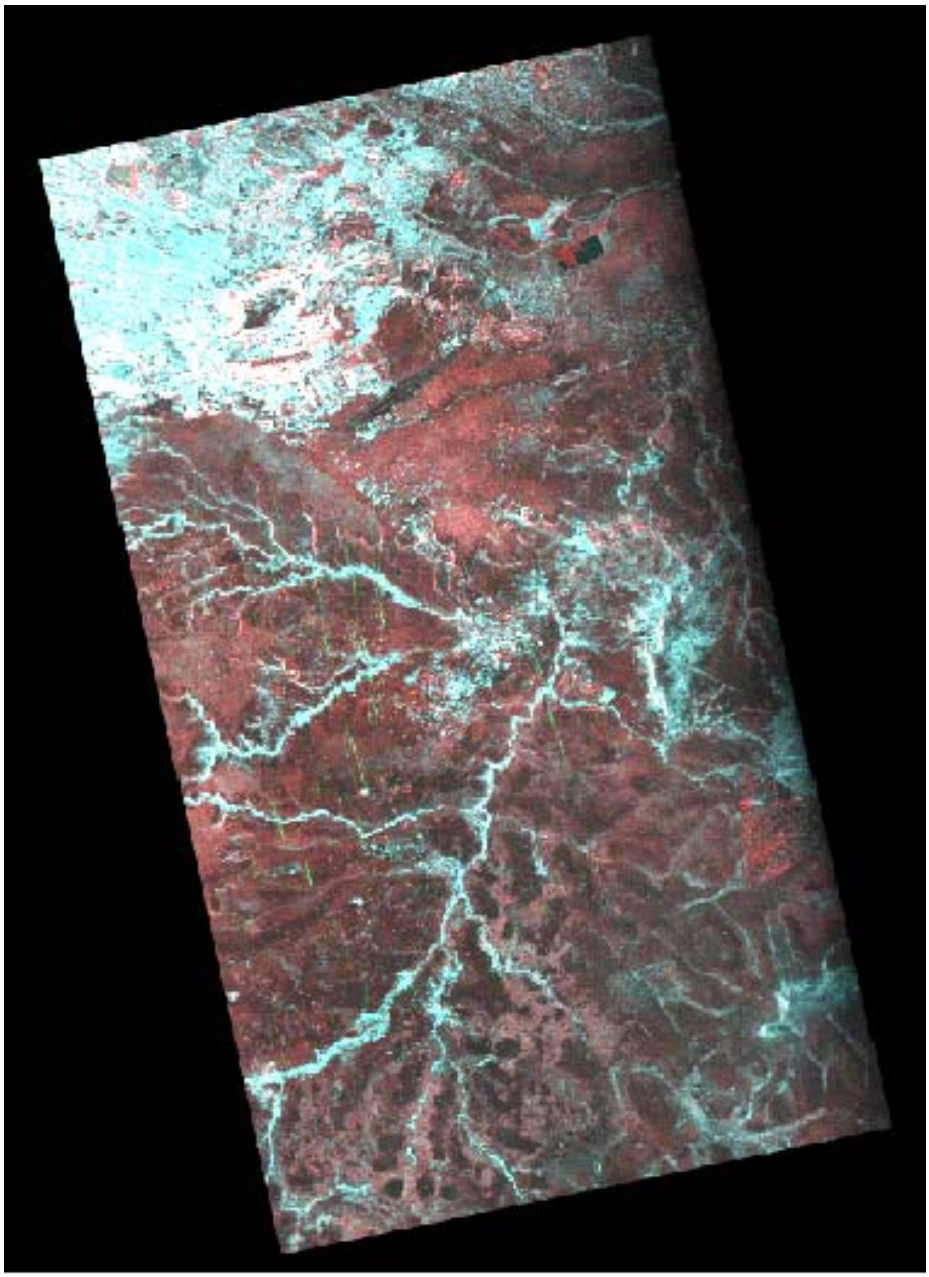

Figure 9: PALSAR image (65 Kilometers by 35Kilometers) for Nairobi, Kenya Acquired May12th, 2007 (polarization-HH, HV and VH; RGB).

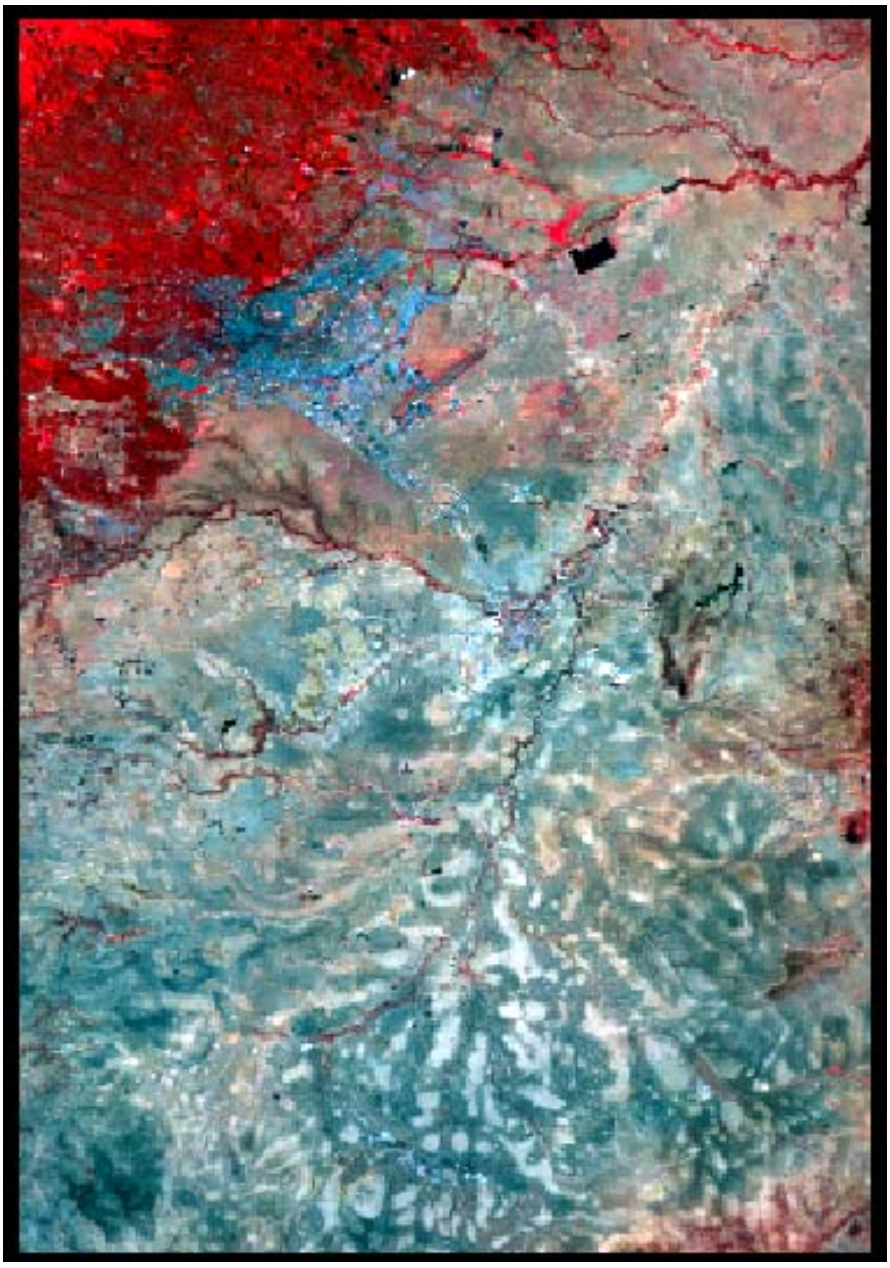

Figure 10: Subsampled Landsat Image for Nairobi, Kenya
Acquired February 1st, 2000 (Bands 4-3-2 RGB).

The major urban developments in this region are around the city of Nairobi, seen in the top left corner of images. With the exception of residential and urban areas in Nairobi, there are no other major cities in this study site. The residential areas have a

vibrant turquoise tone as seen in the radar image (Figure 9). Most of these residential areas have a number of trees in close proximity which strengthens the radar signals. The presence of trees in residential areas can also be validated by looking at the top left corner of the Landsat image (Figure 10), where there are vibrant red tones. These red tones are correlated to the high reflectance of the infrared bands due to chlorophyll in the leaves.

The urban features provide extremely high backscatter resulting in a saturated white tone as seen on the radar image (Figure 9). The presence of cultural features such as buildings and houses in an urban setting strengthens the radar returns resulting in the bright areas. The urban areas in this part of the world are highly congested, particularly in cities such as Nairobi, which makes the return signal stronger for this study site as compared to another urban setting.

Land cover/use further south of Nairobi is typical of the overall landscape of this region. The terrain in this part of Kenya is quite rugged, and this is one of the reasons for the drastic variation in the backscatter on the radar image. As seen in Figure 9, there are a number of dark spots on the image, these are bare ground surfaces which act in a specular manner reflecting energy away from the sensor, this results in little energy making its way back to the sensor and hence the relatively darker spots. The light red and pink tones throughout the radar image are caused by backscatter from grass or other similar ground cover vegetation, which has a texture that returns more energy back to the sensor. In this study these areas of red tones are categorized as savanna. These savannas make up the Nairobi National Park, which is south of the city. Given the fact that the radar image was acquired in the rainy season, the savanna areas are quite healthy. These

healthy savannas areas are not seen on the Landsat image, as it was acquired in the dry season.

The turquoise tones seen in the central region of the radar image are caused by trees which are in close proximity to small streams and rivers. The main river in this area is the Nairobi River, which has a number of tributaries. Along these tributaries there is a high return of the radar signal resulting in the vibrant turquoise. These high returns from the trees in proximity to water bodies shows a clear pattern of riparian vegetation which is easily delineated from the surrounding areas as seen in Figure 9.

Residential and urban areas are easily visible on the Landsat image (Figure 10). Residential areas have a vibrant red tone, and can be seen in the top left corner of the image. Urban areas appear to have a dark blue tone. Particularly the city of Nairobi can be easily detected (top left) on the image, as it has a unique blue tone.

Bare grounds can be seen all throughout the Landsat image (Figure 10). They appear to have a cream tone and unique geographic shapes. The bare ground class is more prominent further south of Nairobi, particularly towards the bottom of the Landsat image. Savannas are visually harder to see on the Landsat image as they have a light pink tone; however, they can be seen along the top right corner of the Landsat image.

4.0 Analysis and Results

The next sections present the finding of the three study areas. The methodology for each section is common to all three study areas. This methodology included the evaluation of original radar, followed by radar texture, fusion of radar texture, Landsat and sensor fusion. Each of the datasets (radar and Landsat TM), have been analyzed separately and in combination with each other. Having a set methodology for all three study areas helped analyze the results in more detail, and also provided a more accurate representation for each of the three areas.

4.1 Bangladesh

The first study site to be evaluated is Bangladesh. The next few sections discuss the findings for the radar and Landsat datasets. Both datasets were evaluated independently and in combination with each other.

4.1.1 Original Radar

Prior to undertaking any analysis and subsetting the data, it is often useful to look at statistical values for the data. Examining the mean and standard deviation of spectral signatures for different land covers/uses can provide unique and validating information about the image. Spectral signatures for the four areas of interest (AOIs) were extracted and their statistics are presented in Table 2.

Table 2: AOI class statistics (DN values) from PALSAR scene. Mean and Standard Deviation.

Land Cover/Use Classes	**Band's**				
		HH	**HV**	**VH**	**VV**
Water	$\overline{X}$ σ	7.5 6.4	7.3 5.4	6.8 5.2	7.5 6.6
Agriculture	$\overline{X}$ σ	16.4 7.0	17.8 7.5	16.4 7.2	14.9 6.8
Residential	$\overline{X}$ σ	31.0 14.6	42.0 16.8	39.4 16.1	27.0 12.5
Forest	$\overline{X}$ σ	19.7 8.5	25.6 10.3	24.4 9.8	16.4 7.5

Water as expected has low Digital Number (DN) values for all four polarizations, primarily because it acts in a specular manner, reflecting energy away from the sensor resulting in low backscatter. Water can easily be delineated from the surrounding land covers due to its low backscatter properties as seen in Figure 3. The lower left corner of the image is the approximate area where the Ganga and Jamuna rivers converge.

Agriculture also has low DN values. This is because the imagery date was during the sowing season, and crops (primarily rice) have not fully matured resulting in low backscatter. If the image had been acquired later in the growing and harvesting season for rice, the radiometric response would have been higher.

The high DN values for residential areas were what would be expected of any area with a number of cultural features such as houses. In Figure 3, high backscatter for the residential areas can be seen. This is related not only to the presence of trees, but also

due to slanting tin roof structures. As mentioned earlier, these slanting roof structures strengthen the radar backscatter. Cross polarization DN values for residential areas are higher when compared to like polarization. This relates to the phenomenon of measuring both amplitude and phase differences, rather than looking only at one component of the returned signal as is the case in like polarization. The residential areas have a high standard deviation, indicating the complexity of these features.

Similarly, DN values for forest, particularly cross polarization, are higher as compared to like polarization. The DN values for like polarization would have been higher if a different type of forest was selected. Forests in this study are identified as mangroves, and due to the presence of water the radar signal might be muted, resulting in low DN values.

4.1.1.1 Transformed Divergence

The next step in the analysis prior to undertaking classification is to evaluate the separability among the four classes. Evaluating TD values provides a framework for selecting the best bands for land cover classification. TD has been consistently used to not only evaluate separability, but has also proved useful in eliminating many of the redundancies of multiple classifications.

Transform Divergence values for original PALSAR data are presented in Table 3. TD values for most class pairs are satisfactory (>1,500), with the exception of a few class pairs in like polarization (HH and VV).

Table 3: TD values for original radar scene, PALSAR. (Res = residential, Ag =agriculture).

Bands	Avg.	Min.	Water-Res	Water-Ag	Water-Forest	Res-Ag	Res-Forest	Ag-Forest
HH	1345	140	2000	1664	1939	1411	917	140
HV	1820	1100	2000	1883	2000	1998	1936	1100
VH	1832	1214	2000	1961	2000	1998	1919	1214
VV	1108	34	1997	1163	1470	1120	863	34

As expected, water is highly separable from all other classes, primarily due to its specular characteristics resulting in low backscatter. On average water has a TD value of 1,839 when paired with other classes.

The residential-agricultural class pair has a low separability for HH and VV polarization, with an average TD value of 1,265. However, TD values for cross polarization (HV and VH), are much higher with an average of 1,998. This is an increase of over 58% within the same class pair (residential-agriculture), when comparing cross and like polarization. The high cross polarization TD values for this class pair can be validated by looking at the DN values in Table 2. The DN value differences within cross polarization are higher for residential and agriculture, as compared to like polarization.

Similarly, when comparing separability between the residential-forest class pair, TD values for like polarization are much lower as compared to the cross polarization (Table 3). There is an increase of over 100% in the TD values for the two classes, this too can be validated by looking at the statistical values (Table 2) which are significantly different from each other. Forests have higher DN values as compared to agriculture, making them highly separable using cross polarization.

TD values for the agriculture-forest class pair are very low in all four original radar polarizations. The class pair has a TD value of 140 and 34 for the HH and VV polarization, bringing the average for like polarization to 87, which indicated no separability. On the other hand, cross polarization has a relatively higher average TD value of 1,157 for the cross polarization HV and VH, but it is still not sufficient for successfully separating the two classes. Theoretically, agriculture and forest would be highly separable; however, the DN values for the two land covers/uses are similar as seen in Table 2, resulting in low TD values.

4.1.1.2 Radar Classification

In order to derive the classification for the four classes a maximum likelihood decision rule was applied to the original radar dataset. The maximum likelihood decision rule was not only applied to single bands, but also multiple band combinations. Combinations for multiple bands were based on the classification accuracy of individual bands. To access the accuracy for classification, the classified pixels for the four classes were compared to areas of truth or validation sites. Two truth sites for each land cover/use were delineated.

The classification results for the original radar data have been summarized in Tables 4, 5 and 6. The classification accuracies for all four individual bands are quite good, ranging from 76% to 89%. However, when all four bands are combined the overall classification accuracy increases to 91% (Table 6).

Table 4: Classification accuracies for individual radar bands (HH and HV), Bangladesh.

PALSAR band HH					**Users Accuracy**
Land covers/uses	Water	Res	Ag	Forest	
Water	**16258**	1	441	360	**95.3**
Res	2	**5162**	319	255	**90.0**
Ag	7	1536	**2334**	902	**48.8**
Forest	19	48	2067	**832**	**28.1**
Producers Accuracy	**99.8**	**76.5**	**45.2**	**35.4**	
Overall Accuracy					**80.5**
PALSAR band HV					**Users Accuracy**
Land covers/uses	Water	Res	Ag	Forest	
Water	**16263**	0	849	62	**94.7**
Res	0	**6333**	40	254	**95.6**
Ag	28	26	**3655**	1288	**73.1**
Forest	0	388	617	**745**	**42.6**
Producers Accuracy	**99.8**	**93.9**	**70.8**	**31.7**	
Overall Accuracy					**88.4**

There is a direct relationship between the classification accuracies and TD values. The HV and VH bands yielded the best separability (Table 3), and hence resulted in the best accuracies among the four bands.

Water, as expected, resulted in excellent classification accuracies across all individuals and four stacked bands. These high classification accuracies for water can be validated by not only looking at the statistical values (Table 2), but also the separability values (Table 3). Water has low DN values (Table 2) as compared to other land covers/uses making it highly separable. This highly separable characteristic is initially reflected in the TD value and eventually resulted in high classification accuracies.

Table 5: Classification accuracies for individual radar bands (VH and VV), Bangladesh.

PALSAR band VH					**Users Accuracy**
Land covers/uses	Water	Res	Ag	Forest	
Water	**16210**	0	583	44	**96.3**
Res	0	**6269**	59	275	**94.9**
Ag	81	42	**3965**	1323	**73.3**
Forest	0	436	554	**707**	**41.7**
Producers Accuracy	**99.5**	**92.9**	**76.8**	**30.1**	
Overall Accuracy					**88.9**
PALSAR band VV					**Users Accuracy**
Land covers/uses	Water	Res	Ag	Forest	
Water	**16264**	4	1326	706	**88.9**
Res	0	**4655**	1073	109	**79.7**
Ag	2	1852	**1324**	620	**34.9**
Forest	9	236	1438	**914**	**35.2**
Producers Accuracy	**99.9**	**69.0**	**25.7**	**38.9**	
Overall Accuracy					**75.8**

Table 6: Classification accuracies for stacked radar bands (HH, HV, VH, VV).

PALSAR band HH, HV, VH, VV					**Users Accuracy**
Land covers/uses	Water	Res	Ag	Forest	
Water	**16236**	0	280	24	**98.2**
Res	2	**6277**	95	226	**95.1**
Ag	16	91	**3676**	624	**83.4**
Forest	37	379	1110	**1475**	**49.2**
Producers Accuracy	**99.7**	**93.0**	**71.2**	**62.8**	
Overall Accuracy					**90.6**

Residential land cover/use is always relatively heterogeneous in nature, particularly in countries similar to Bangladesh. Residential land cover/use in this part of the region encompasses small agricultural fields and also trees. The classification

accuracies for residential land cover/use range from 69% to 94% for individual radar bands, and is 93% for all four bands taken together. The classification accuracy of 69% was in the VV band, and this is directly reflective of the poor separability (Table 3) in the TD analysis. The high classification accuracies (94% and 93%) are seen in the cross polarization (HV and VH) bands. This again can be validated by looking at the separability values, where both HV and VH bands yielded a TD value of over 1,900.

The classification accuracies for the agricultural class ranged from 26% to 77%, for the individual bands and 71% for all four bands. Cross polarization (HV and VH), were the only two individual bands that had an accuracy of over 70%. The like polarization bands, HH and VV, had extremely low accuracies of 45% and 26%. This variability in accuracies is again reflective of the separability values. Agriculture when paired with other classes, particularly forest, had exceptionally low separability (140 and 34) values for HH and VV bands, in turn resulting in poor classification.

The agriculture class was among the few land covers/uses that had low classification accuracies. As seen in the classification tables, many agricultural land cover/use pixels have been misclassified. The majority of the misclassified pixels were from the forest class. This is directly related to topography and the heterogeneous landscape. Most of the agricultural fields in this part of Bangladesh have a number of trees in close proximity, resulting in misclassification. This type of misclassification is referred to as error of omission or under classification of the agricultural class (Herold, 2000). Misclassification occurs when pixels that should have been classified as

agriculture get assigned to forest or other classes, resulting is low classification accuracies and reliability.

Forest had the lowest classification accuracies of all four classes. The classification accuracies ranged from 30% to 39% for the individual bands, and 63% when all individual bands were combined. These accuracy values are exceptionally low and are not satisfactory for classification purposes. The majority of misclassification was with agriculture, i.e., pixels that should have been classified as forests were misidentified as agriculture. This misclassification is a result of the heterogeneous nature of the landscape.

The DN values for forest and agriculture are quite similar to each other, and this in turn results in low separability among the two land covers. The result of similar DN values and low separability is reflected through the poor classification accuracies for the forest class.

Overall, based on the classification results of individual and stacked original bands, cross polarization (HV and VH), yielded the best accuracies as compared to like polarization (HH and VV). This trend of cross polarization yielding better results is also the case for TD when evaluating the separability results. Similar to the classification accuracies, cross polarization yielded higher separability as compared to like polarization.

Regardless of the number of bands and polarizations, certain classes such as forest had extremely low classification accuracies. Even when all four radar bands are stacked together, the classification accuracies for the forest class were low (63%). However for

agriculture, when all bands are stacked the classification accuracies increase to 71% from 45% (HH) and 26% (VV). In general, all four bands stacked together yield higher classification accuracies, as opposed to each band taken individually.

Based on past research, the overall classification accuracies can be increased by combining the best two and three band combinations. To evaluate the effectiveness of this technique; the best bands were combined based on their individual classification accuracies. The primary intent here was to determine if combining individual bands yielded higher classification accuracies as opposed to taking them individually (Table 7).

Table 7: Classification accuracies, best two and three band combinations, Bangladesh.

Best Two Bands (HV and VH)					**Users Accuracy**
Land covers/uses	Water	Res	Ag	Forest	
Water	**16218**	0	655	39	95.9
Res	4	**6336**	90	295	94.2
Ag	69	27	**3786**	1261	73.6
Forest	0	384	630	**754**	42.6
Producers Accuracy					
	99.6	**93.9**	**73.4**	**32.1**	
Overall Accuracy					**88.7**
Best Three Bands (HH, HV and VH)					**Users Accuracy**
Land covers/uses	Water	Res	Ag	Forest	
Water	**16265**	0	558	28	96.5
Res	3	**6318**	79	245	95.1
Ag	12	77	**3732**	865	79.6
Forest	11	352	792	**1211**	51.2
Producers Accuracy					
	99.8	**93.6**	**72.3**	**51.6**	
Overall Accuracy					**90.1**

Considering that HH, HV and VH yielded the highest classification accuracies when they have been stacked together. The classification accuracies for the best two band

combinations show marginal improvements over each band (HV and VH) taken individually. The overall classification for the two bands taken individually was at 89%. However, when a third band (HH) is added to the two band combination the overall accuracy increases to 90%, which is relatively higher than each band taken individually. The addition of an extra band does validate the fact that adding bands does indeed increase the overall classification accuracies.

4.1.2 Radar Texture

A total of four different texture measures (variance, skewness, mean euclidean distance, and kurtosis) at four window sizes ranging from 5 x 5 to 13 x 13 were evaluated for this study site. An evaluation of TD values for each of the four different texture measures is followed by a classification accuracy assessment of the best texture measure and window size.

4.1.2.1 Variance

Variance texture measure was calculated for the original radar data, using multiple window sizes. In Table 8, there is a significant increase of the TD values after variance texture is applied to the original radar image. The 7 x 7 window size yielded the best results when compared to the other three window sizes (5 x 5, 11 x 11, and 13 x 13).The use of variance texture is appropriate for class pairs in like polarization where original radar TD values are lower as compared to cross polarization.

Class pairs for agriculture-forest, which were inseparable using the original radar, are highly separable after applying variance texture at the 5 x 5 and 7 x 7 window sizes.

Similarly, the separability between other class pairs including water-agriculture, water-forest, and residential-agriculture all show improvements in TD values.

Table 8: TD values for variance texture, Bangladesh.

Bands	Avg.	Min	Water-Res	Water-Ag	Water-Forest	Res-Ag	Res-Forest	Ag -Forest
TD values (5x5 Texture) for Bangladesh, PALSAR image								
HH	1900	1734	2000	1800	2000	2000	1868	1734
HV	1998	1986	2000	2000	2000	2000	2000	1986
VH	1998	1986	2000	2000	2000	2000	1996	1986
VV	1873	1500	2000	1895	2000	2000	1841	1500
TD values (7x7 Texture) for Bangladesh, PALSAR image								
HH	1932	1821	2000	1821	2000	2000	1906	1867
HV	2000	2000	2000	2000	2000	2000	2000	2000
VH	2000	2000	2000	2000	2000	2000	2000	2000
VV	1909	1626	2000	1936	2000	2000	1893	1626
TD values (11x11 Texture) for Bangladesh, PALSAR image								
HH	1779	1478	2000	1568	2000	2000	1626	1478
HV	2000	1999	2000	2000	2000	2000	2000	1999
VH	2000	1999	2000	2000	2000	2000	2000	1999
VV	1722	911	2000	1780	1999	1999	1643	911
TD values (13x13 Texture) for Bangladesh, PALSAR image								
HH	1513	819	2000	1117	1994	1981	1170	819
HV	1998	1987	2000	2000	2000	2000	2000	1987
VH	1997	1983	2000	2000	2000	2000	2000	1983
VV	1428	359	2000	1235	1921	1901	1155	359

The class pair agriculture-forest had a TD value of 34 (Table 3) in the original VV band and with the use of texture one can see an improvement of 1,592, yielding a TD value of 1,626 (Table 8). Similarly TD values in the HH band for the same class pair (agriculture-forest) increased by over 1,727, resulting in a TD value of 1,867. The TD values for cross polarization also showed improvements, when compared to the original radar data with the 7 x 7 texture window size.

The use of texture on the two class pairs of water-agriculture and residential-agriculture yielded higher separability, particularly for like polarization. There is an increase of 773 for the VV polarization in the water-agriculture class pair and an increase of 157 in the HH polarization. There is also an increase of 589 (VV) and 880 (HH) for the class pair of residential-forest after applying texture on the original radar image. The residential-forest pair also showed major improvement in the separability values, with an increase of 989 for the VV polarization and 1,030 for HH polarization.

There are certain patterns which emerge when multiple texture window sizes are used. As the window size increases, average TD values also increase, however the values start to decrease at the 11 x 11 window size as seen in Table 8. Similar results were also observed in previous studies conducted by Idol et al. (2007) where the TD values saturate at a particular window size, and reduce thereafter.

This trend of TD values saturating at a particular window size and decreasing thereafter is related to the pixel size and also the ground feature characteristics. A larger texture window size correlates to an increased number of pixels being included during computation of the TD values. Taking into account the heterogeneous nature of the study site, an increased number of pixels within a larger texture window did not yield better results.

4.1.2.2 Skewness, Mean Euclidean Distance, and Kurtosis

Table 9, summarizes the average TD values for the other three texture measures, skewness, mean euclidean distance, and kurtosis. All average TD values for these texture

measures are exceptionally low as compared to variance texture. Considering that these texture measures are not capable of successfully distinguishing the land covers/uses, they will not be used for classification purposes. With the exception of mean euclidean distance, none of the other texture measures had TD values of over 1,500. As a larger window size was used, the average TD values increase, however the values were still well below 1,500 and would have yielded poor classification accuracies. The low TD values for these texture measures, was validated by looking at the images. There appears to be a substantial loss of textural information, which in turn makes the images appear washed out and pixilated resulting in poor separability among the classes.

Table 9: TD values for the remaining texture measures, Bangladesh.

Bands	Avg.	Min	Avg.	Min	Avg.	Min	Avg.	Min
Skewness Texture Measure								
	5x5		7x7		11x11		13 x13	
HH	841	177	926	253	998	328	1012	302
HV	797	82	884	97	1010	117	1049	123
VH	786	69	868	79	967	93	994	92
VV	878	169	983	263	1066	368	1084	396
Mean Euclidean Distance								
	5x5		7x7		11x11		13 x13	
HH	1051	153	1053	170	1086	205	1096	218
HV	1380	479	1449	591	1530	745	1555	796
VH	1378	495	1446	603	1528	755	1555	807
VV	882	78	916	81	937	88	942	90
Kurtosis								
	5x5		7x7		11x11		13 x13	
HH	18	1	42	5	103	0	142	0
HV	0	0	0	0	89	0	239	0
VH	0	0	0	31	114	0	287	16
VV	23	2	72	0	180	27	231	23

4.1.2.7 Radar Texture Classification

Variance texture measure yielded the best separability results, and hence it is selected for the next step of classification. In particular it was the 7 x 7 variance texture that showed the most improvements over the original radar dataset. Classification was performed on each individual texture band, four stacked bands and also the best two and three band combinations.

For the individuals band HH, the overall classification after applying texture reduced to 68% (Table 10) from an original 80%. Most surprising was the drop in producers accuracy for the forest class for the HH band, which went from 35% in the original dataset to 5%, after texture was applied. Similarly, classification accuracies for the other three classes (water, residential and agriculture), also decreased, after texture was applied.

Table 10: Classification accuracies variance texture 7x7 (HH and HV), Bangladesh.

HH radar texture					**Users Accuracy**
Land covers/uses	Water	Residential	Agriculture	Forest	
Water	**7728**	0	1722	1059	73.5
Residential	0	**3963**	0	105	97.4
Agriculture	79	2088	**3297**	1058	50.6
Forest	38	696	142	**127**	12.7
Producers Accuracy	**98.5**	**58.7**	**63.9**	**5.4**	
Overall Accuracy					**68.4**
HV radar texture					**Users Accuracy**
Land covers/uses	Water	Residential	Agriculture	Forest	
Water	16207	0	1462	226	90.6
Residential	0	5008	13	102	97.8
Agriculture	0	62	3513	1536	68.7
Forest	0	1677	173	485	20.8
Producers Accuracy	**100.0**	**74.2**	**68.1**	**20.6**	
Overall Accuracy					**82.8**

The classification accuracies for the other three individual bands VV, HV and VH all reduced when texture was applied. The classification accuracies for certain classes reduced more than others, for example, forest has low classification accuracies for all bands in the original radar and texture datasets. However, in the VV band the producers accuracy drops to 0.3% from 39% when texture is applied. This was the most drastic drop among all classes after texture was applied (7 x 7).

Table 11: Classification accuracies variance texture 7 x 7 (VH and VV), Bangladesh.

VH radar texture					**Users Accuracy**
Land covers/uses	Water	Residential	Agriculture	Forest	
Water	16241	0	1770	208	89.1
Residential	0	5083	11	115	97.6
Agriculture	0	42	3161	1507	67.1
Forest	0	1622	219	519	22.0
Producers Accuracy	**100.0**	**75.3**	**61.2**	**22.1**	
Overall Accuracy					**82.0**
VV radar texture					**Users Accuracy**
Land covers/uses	Water	Residential	Agriculture	Forest	
Water	5106	84	1384	1576	62.7
Residential	0	2879	56	16	97.6
Agriculture	47	3642	3649	749	45.1
Forest	0	142	72	8	3.6
Producers Accuracy	**99.1**	**42.7**	**70.7**	**0.3**	
Overall Accuracy					**60.0**

The classification accuracies for most classes reduced after texture was applied with the exception of agriculture. The use of texture on like polarization (HH and VV) were the only two bands that helped increase the producers accuracy for agriculture. The

producers accuracy increased to 64% (HH) from 45% and also for the VV band they increased to 71% from 26% in the original radar dataset.

A similar pattern was also found when evaluating all four (HH, HV, VH and VV) texture bands (Table 12). The overall classification accuracy for variance texture drops to 85% from 90% when all bands are combined. However, the producers accuracy for agriculture increased 2%, when all four bands were combined.

Table 12: Classification accuracies for stacked variance texture bands.

HH, HV, VH, VV					**Users Accuracy**
Land covers/uses	Water	Residential	Agriculture	Forest	
Water	**16167**	0	1273	318	91.0
Residential	0	**5354**	1	106	98.0
Agriculture	117	303	**3800**	1353	68.2
Forest	6	1090	87	**572**	32.6
Producers Accuracy	**99.2**	**79.4**	**73.6**	**24.4**	
Overall Accuracy					**84.8**

Table 13 shows the classification accuracies for the best two and three band combinations. The classification accuracies for the two band combination comprise of HV and VH as the best two band combination in the original radar dataset. However, the classification values after applying texture decreased to 83% from an original 88**%.** The classification accuracies for the three band combinations dropped to 84% from an original 90%.

Table 13: Classification accuracies for best two and three band combination texture, Bangladesh.

Best two bands (HV VH)					**Users Accuracy**
Land covers/uses	Water	Residential	Agriculture	Forest	
Water	16288	0	1514	181	90.6
Residential	9	5025	3	67	98.5
Agriculture	2	616	3458	1646	60.4
Forest	0	1106	186	455	26.0
Producers Accuracy					
	99.9	**74.5**	**67.0**	**19.4**	
Overall Accuracy					82.6
Best three bands (HH, HV and VH)					**Users Accuracy**
Land covers/uses	Water	Residential	Agriculture	Forest	
Water	16219	0	1546	267	89.9
Residential	0	5420	1	64	98.8
Agriculture	71	590	3449	1560	60.8
Forest	0	737	165	458	33.7
Producers Accuracy					
	99.6	**80.3**	**66.8**	**19.5**	
Overall Accuracy					83.6

Surprisingly, the use of texture was able to improve the overall separability among the classes. However, it was not very efficient in improving the overall classification accuracies. For most bands the use of texture reduced the overall classification accuracies. This was surprising considering that variance texture greatly improved the overall TD values, it should have shown moderate improvements in overall classification accuracies. Previous studies (Haack, 2007) which focused on land covers/uses classification have shown improvements in classification accuracies after variance texture was applied. This however was not the case for this particular study area. One speculation for this might have to do with edge pixels being incorrectly classified

after texture is applied. Pixels along the boundary of an AOI might have been misclassified, resulting in lower accuracies.

4.1.3 Radar Fusion: Original Radar with Radar Texture

Original radar data were combined with variance texture. The intent was to determine if the overall classification accuracies can be improved further by adding texture bands to the original radar bands.

Considering that 7 x 7 variance texture provided the highest separability among the classes, it is beneficial to examine the results obtained from fusing the two datasets, i.e., original radar with the 7 x 7 texture. Table 14, summarizes the classification accuracies for the two datasets, where all four bands are fused together. There is a marginal improvement in the overall classification accuracies. The overall accuracies increase to 92% from 90% (original radar) and 85% (variance texture). The producers accuracy for agriculture showed the most improvement increasing from 71% (original radar) and 74% (variance texture) to 90%. However, the producers accuracy for forest reduced to 35% as compared to the 63% in the original radar dataset.

Table 14: Classification accuracies for original radar with radar texture (variance7x7), Bangladesh.

HH, HV, VH,VV					**Users Accuracy**
Land covers/uses	Water	Res	Ag	Forest	
Water	16180	0	376	47	97.5
Res	0	6286	5	116	98.1
Ag	42	53	4668	1363	76.2
Forest	69	408	112	823	58.3
Producers Accuracy	**99.3**	**93.2**	**90.4**	**35.0**	
Overall Accuracy					**91.5**

Overall, the fusing of the original radar datasets with radar variance texture did show minor improvements. However, there are certain land cover/use such as forest that have lower classification accuracies (below 70%). Even though the classification accuracies for variance texture did not yield good results, the combined accuracies for original radar and radar texture do look promising.

4.1.4 Landsat Thematic Mapper

The Landsat sensor has been the source for many land cover/use classification practices. This section will explore its capabilities and efficiency to classify land covers/uses in Bangladesh.

Prior to evaluating classification accuracies using the Landsat sensor, it is essential to examine the statistical values. Similar to the original radar dataset, these DN values provide validating information, useful when examining the separability and classification results.

Table 15 contains the statistical values for spectral signatures extracted from the same AOIs using the TM image. There are certain anomalies in these DN values, particularly when looking at the standard deviation for water. Water would be expected to have low standard deviations across all bands, however, this was not the case for this study area. The mean values for water are quite similar to other studies conducted in the past, with the exception in the second MIR (mid infrared) band, where the mean is low and standard deviation is comparatively higher. These anomalies might have been caused by the presence of plankton, sediments or aquatic vegetation.

Table 15: AOI class statistic (DN values), from TM image. Mean and Standard Deviation, Bangladesh.

Land cover/use		**Bands**					
		Blue	**Green**	**Red**	**NIR**	**MIR**	**MIR**
Water	$\overline{X}$	67.9	54.1	50.6	41.6	44.0	24.8
	σ	6.6	8.3	12.9	16.4	26.7	23.9
Residential	$\overline{X}$	58.9	45	39.1	63.1	47.1	28.7
	σ	2.0	2.4	3.9	5.9	7.7	6.8
Agriculture	$\overline{X}$	57.1	44.5	37.2	77.2	49.5	27.7
	σ	2.7	3.3	5.7	10.4	10.5	8.6
Forest	$\overline{X}$	58	45.7	43.6	66.5	62.7	39.8
	σ	2.3	3.2	7.0	5.93	13.1	12.4

Residential areas have high DN values for the NIR (near infrared) band, because of the combination of trees, garden plots, and metal rooftops. In particular, it is the sensitive nature of infrared bands to the chlorophyll level in vegetation which yields high DN values across all bands and classes.

Similarly, the NIR band has the highest DN value for agriculture. One of the difficulties of using this Landsat imagery is the similarity between DN values for residential and agriculture land covers/uses, particularly when both classes are heterogeneous (Table 15). DN values for these land cover types are not separable which potentially might cause a problem during classification and accuracy assessment, due to misclassification of pixels.

Forest cover has a high DN value across all infrared bands, due to the responsive nature of the infrared wavelengths towards healthy green vegetation. The DN value for forest indicates that it would be highly separable from the agriculture and residential, particular when using the two mid infrared bands.

The visible bands, particularly the blue band has high DN values for all four classes. This is due to its short wavelength, which is most sensitive to reflection and scattering in the upper atmosphere due to the presence of moisture or clouds, resulting in some energy being reflected back to the sensor. Longer wavelengths, such as infrared are capable of penetrating these atmospheric conditions and in turn are more directly related to the ground conditions as compared to the shorter visible wavelengths.

4.1.4.1 Transformed Divergence

Table 16 summarizes separability results for the Landsat TM dataset. With exception of the first MIR band, water is highly separable when paired with residential and agriculture. The low TD values for water in the first MIR band is related to their (agriculture and residential) statistical DN values found in Table 16. The water AOI has high DN values in the visible bands, however its DN values for both MIR bands (44 and 25) are very similar to the DN values for residential (47 and 29) and agriculture (49 and 28), hence resulting in zero separability, as seen in Table 16. In particular, high standard deviation (27) for water in the first MIR band (Table 16) can be linked to the 0 TD values.

Table 16: TD values for Landsat image, Bangladesh.

Bands	Avg.	Min	Water-Res	Water-Ag	Water-Forest	Res-Ag	Res-Forest	Ag-Forest
Blue	1135	116	1998	2000	2000	522	116	176
Green	1117	189	2000	2000	1999	189	196	320
Red	1564	453	1999	2000	1676	453	1504	1756
NIR	1393	138	1944	1999	1974	1384	138	918
MIR	1036	0	0	0	1990	408	1977	1843
MIR	1367	79	1749	1747	746	79	1928	1952

The residential-agriculture class pair has low separability across all six bands, making them inseparable. The highest TD value for the class pairs was 1,384 in the NIR band. It is the end of the dry season, and many agricultural fields are still fallow and have poor vegetation making them spectrally similar to residential areas.

This is one of the difficulties of using an optical sensor, it is unable to efficiently differentiate between fallow agriculture and residential land covers/uses. This is indicated by low separability values for the residential-agriculture class as seen in Table 16. The DN values (Table 15) for agriculture and residential are similar to each other, hence validating the low separability for this particular class pair. If the same AOIs were used on imagery acquired during the monsoon and harvesting seasons, TD values would have been much higher for this class pair. Imagery acquired during the monsoon season would have had healthier vegetation, resulting higher DN values for agriculture. Ideally the presence of more vegetation on the agricultural fields would have resulted in both classes having unique DN values, resulting in high separability.

TD values for the fifth class pair; residential-forest are also lower than expected. Unlike the TD values for the previous class pair, residential-agriculture, both MIR bands yield good separability for residential-forest. The first MIR band has a TD of 1,977 and the second 1,928. However, the NIR band has a TD of only 138 as compared to 1,384 in the previous class pair for residential-agriculture. The red visible band had a TD of 1,504 as compared to 453 for residential-agriculture. Once again the DN values in Table 15 for residential and forest are also quite similar to each other, with the exception of NIR and the red visible band which are significantly different. These variations in DN values for

residential and forest land cover/use, are directly related to the low TD values for this class pair.

TD values for the last class pair, agriculture-forest were relatively higher as compared to the previous two classes. The MIR bands had TD values of 1,843 and 1,952; however, the NIR band had a TD value of only 918. The value for the NIR band was predicted to be higher because the DN value for agriculture was 77 and 66 for forest, which should have resulted in higher separability. The red visible bands had a TD value of 1,756 providing excellent separability for the class pair.

4.1.4.2 Classification Landsat Image

The next step in the analysis was to stack all six (blue, green, red, NIR, MIR, and MIR) Landsat bands together and evaluate the classification accuracies. Table 17 summarizes the classification accuracies for all four classes. The accuracies from the stacked Landsat bands show significant improvement when compared to the original radar and radar texture bands.

Table 17: Classification accuracies Landsat image, Bangladesh.

Blue, green, red, NIR, MIR, NIR bands					**Users Accuracy**
Land covers/uses	Water	Res	Ag	Forest	
Water	**15731**	75	0	8	99.5
Res	2	**5725**	24	229	95.7
Ag	558	339	**5137**	0	85.1
Forest	0	608	0	**2112**	77.6
Producers Accuracy	**96.6**	**84.9**	**99.5**	**89.9**	
Overall Accuracy					**94**

The overall accuracy (94%) achieved using the Landsat sensor is better than the original four radar (91%) and variance texture (85%) bands stacked together. Of particular interest is the high users and producers accuracy for agriculture and forest. These are two classes which have consistently had the lowest classification accuracies, however, with the use of Landsat their accuracies are both well over 70 %. The producers accuracy for forest is 90%, which is a vast improvement considering that the highest accuracy attained for this class was 62% using all four bands in the original radar dataset. Overall, the results from classifying the Landsat image look promising for future research. All four classes showed major improvements when classified using the optical sensor. Classes such as forest which have been consistently misclassified are now clearly distinguishable.

4.1.5 Sensor Fusion

When comparing classification accuracies for the two original datasets, i.e., radar and Landsat, the Landsat data yields better results. It is evident from the results of this study site, optical data is better suited for classification. The next two sections examine if the overall classification can be improved further by using two fusing techniques, i.e., layer stacking and PCA. The intent is not only to determine if the overall classification accuracies can be increased, but to also document which procedure results in minimal loss of key spectral information.

4.1.5.1 Layer stacking

The next step was to evaluate the classification accuracies for original radar layer stacked with the Landsat dataset. All four original radar bands were layer stacked with the six Landsat bands for this part of the analysis. The classification accuracies for both datasets stacked are summarized in Table 18.

Table 18: Classification accuracies for original radar and Landsat, Bangladesh.

All 10 bands (Four radar and Six Landsat)					**Users Accuracy**
Land covers/uses	Water	Res	Ag	Forest	
Water	**16269**	0	0	2	100.0
Res	0	**6611**	40	11	99.2
Ag	22	33	**5121**	34	98.3
Forest	0	103	0	**2302**	95.7
Producers Accuracy	**99.9**	**98.0**	**99.2**	**98.0**	
Overall Accuracy					**99.2**

There is a vast improvement in accuracies when both datasets are stacked together. The overall accuracy is almost 100%, with all four land covers/uses above 98% producers accuracy. The overall accuracy with the original radar dataset was at 90% and when using the Landsat image by itself was 94%.

The classification accuracies for the two combined datasets provide reliable and validating results. The combination of the two datasets results in not only improved classification accuracies, but also makes the analysis more consistent for all four classes.

The next analysis was to layer stack the radar texture and Landsat images. Considering that the variance texture (window size 7 x 7) measure yielded the highest

separability among the classes, it was used for this part of the analysis. All four bands of radar variance texture were stacked with the Landsat bands. Table 19 summarizes the classification accuracies for the two datasets.

Table 19: Classification accuracy for radar texture (variance7x7) and Landsat, Bangladesh.

Blue, green, red, NIR, MIR, NIR bands					**Users Accuracy**
Land covers/uses	Water	Res	Ag	Forest	
Water	**16195**	0	0	37	99.8
Res	0	**6255**	0	18	99.7
Ag	96	73	**5157**	44	96.0
Forest	0	419	4	**2250**	84.2
Producers Accuracy	**99.4**	**92.7**	**99.9**	**95.8**	
Overall Accuracy					**97.7**

The overall classification accuracies for the radar texture and Landsat (98%) are slightly lower than the previous combination of original radar and Landsat (99%). The accuracies from both these datasets layer stacked are better than the four radar texture bands stacked together (85%) and Landsat alone (94%). The combination of radar texture and Landsat also helps improve the overall consistency and reliability of the classification.

One of the reasons why the overall classification reduced when radar texture and Landsat are stacked is related to the lower accuracies obtained by the radar texture alone. Hypothetically, if the radar variance texture would have yielded higher accuracies for all four classes, the overall accuracy for this dataset (radar texture and Landsat), would have been higher.

4.1.5.2 Principal Component Analysis (PCA)

Next, PCA was used to evaluate the classification accuracies of the three datasets (original radar dataset, radar texture and Landsat). The intent here was to determine if classification accuracies can be increase by combining the principal component from the two datasets, i.e., radar and Landsat. The PCA algorithm is particularly useful for reducing the redundancies in either image by taking only the most dominant spectral characteristic. However, this process of combining the dominant characteristic from either image can result in loss of spectral information.

Similar to the previous section, first original radar data will be analyzed with Landsat data and thereafter radar texture with Landsat. One component of each dataset has been evaluated, as opposed to taking the first three components. The reason for choosing only one principal component was to maintain consistency among all three study sites. Certain land covers/uses had exceptionally poor accuracies when more than one principal component was evaluated. This was true for Bangladesh and Kenya, and hence in order to maintain consistency only one component was taken.

PCA was done on the original four radar bands and then combined with the first PCA of the Landsat bands. The classification results of the original radar PCA and Landsat PCA are summarized in Table 20. The overall classification accuracies for the PCA dataset (94%), is higher than original radar (91%), but there is only an improvement of 0.02% over the original Landsat dataset.

Table 20: PCA of original radar and Landsat image, Bangladesh.

One component					**Users Accuracy**
Land covers/uses	Water	Res	Ag	Forest	
Water	**16281**	0	216	7	98.6
Res	0	**6601**	398	34	93.9
Ag	3	81	**4540**	952	81.4
Forest	7	65	7	**1356**	94.5
Producers Accuracy					
	99.9	**97.8**	**88.0**	**57.7**	
Overall Accuracy					**94.2**

When comparing the two procedures, i.e., layer stacking and PCA, for the same datasets, layer stacking yields higher overall accuracies (99%). This can also be validated by looking at Table 21, where the PCA (one component) of variance radar texture at 7 x 7 window size is combined with the PCA (one component) of Landsat. The overall classification accuracy for this dataset is 94%, which is higher than both original datasets, i.e., radar texture and Landsat. However, when the same date sets are fused together using a simple layer stack the overall accuracies are 98%, which is higher than when using PCA.

Table 21: PCA of Landsat and variance radar texture, Bangladesh.

One component					**Users Accuracy**
Land covers/uses	Water	Res	Ag	Forest	
Water	**16243**	0	410	116	**96.9**
Res	0	**6566**	25	37	**99.1**
Ag	34	148	**4693**	944	**80.6**
Forest	14	33	33	**1252**	**94.0**
Producers Accuracy					
	99.7	**97.3**	**90.9**	**53.3**	
Overall Accuracy					**94.1**

Secondly, in both PCA datasets (Table 20 and Table 21) the producers accuracy for the forest is extremely low (58% and 53%). The producers accuracy for forest in the original radar (71%) and Landsat (89%) datasets was higher as compared to when they were combined using PCA. One of the reasons of this might be the loss of key spectral information during PCA for the two datasets. The loss of key spectral information is one of the major drawbacks of using PCA (Chavez et al. 1991). Based on the results of this study site, layer stacking is a better technique for fusing data from different sensors.

Overall, it can be concluded that the original radar data yielded moderate separability results for the four land covers/uses. However, the use of texture, greatly improved the overall separability among the classes. In particular, it was the variance texture measure at a 7 x 7 window size, which yielded the best TD values. Considering that the variance texture measure showed the most improvement, it was chosen for classification purposes. Surprisingly, the use of radar texture (variance, 7 x 7) did not yield any major improvement in the classification accuracies, but rather reduced the producers accuracies for some classes. On the other hand, the classification accuracies for the Landsat image were better than both the original radar and radar texture. When data from these different sensor (original radar and Landsat) are fused together the classification accuracies were the highest.

4.2 California

The next study to be evaluated was the central valley of California. The same methodology used for Bangladesh was also applied to the California site.

4.2.1 Original Radar

Prior to undertaking the analysis and subsetting the data for the California radar scene, statistical values for AOIs were extracted and are presented in Table 22.

Table 22: AOI class statistics (DN values) from the PALSAR scene. Mean and standard deviation, CA.

Land Cover/Use Classes		**Bands**			
		HH	**HV**	**VH**	**VV**
Almonds	$\overline{X}$	15.42	32.27	35.06	14.11
	σ	7.19	18.24	19.58	6.26
Cotton	$\overline{X}$	7.32	10.44	14.19	7.16
	σ	2.37	2.30	2.98	2.27
Fallow/idle cropland	$\overline{X}$	7.06	10.60	11.80	7.02
	σ	2.10	2.48	2.68	1.96
Alfalfa	$\overline{X}$	12.89	14.86	15.988	12.03
	σ	3.93	4.44	4.78	3.80

Almond plantations have a high DN value for all four polarizations. The DN values for cross polarization are higher, as compared to like polarization. The high DN values for almonds are caused by the strong return signal from the almonds trees which are larger as compared to other crops. Almond trees are in close proximity to each other, which strengthens the radar backscatter resulting in high DN values. The reason for the cross polarization having higher DN values can be attributed to the function of measuring both amplitude and phased difference as opposed to only the amplitude as the case in like polarization.

Cotton and fallow/idle cropland both have very similar DN values. Cotton planting in California starts in March or April and is harvested in September. Considering the time of the year when the radar imagery was acquired (May), the crop had not fully matured and hence the radar returns are weak. Similarly, for the fallow/idle cropland the

radar signal is weak, because there is not much present on the ground to return the signal, acting almost specularly. This low backscattering property of the ground surface results in both cotton and fallow/idle cropland having similar DN values. The similarity in DN values for both these land covers/uses can result in misclassification and low separability.

Alfalfa has high DN values across all four polarizations. Given the time of the year, the alfalfa crop had matured and resulted in high backscatter, providing the high DN values. In this part of the country the farming practices are quite intense and alfalfa fields are dense. A dense alfalfa crop results in a rough texture on the radar image and returns high DN values.

4.2.1.1 Transformed Divergence (TD)

The next step in the analysis was to evaluate the separability values for each of the four classes. Table 23, summarizes the TD values for the each of the four land covers/uses based on the individual bands.

Table 23: TD values for original radar scene, PALSAR, CA.

Bands	Avg.	Min	Almonds-Cotton	Almonds-Fallow	Almonds-Alfalfa	Cotton-Fallow	Cotton-Alfalfa	Fallow-Alfalfa
HH	1068	40	1012	1945	500	1325	40	1583
HV	1180	124	1998	2000	1975	124	284	699
VH	1152	149	1994	2000	1978	184	149	606
VV	925	0	559	1879	327	1399	0	1445

Almonds and cotton are highly separable using cross polarization because almonds have a much higher DN value as compared to cotton. Almonds-fallow/idle and almonds-alfalfa are also quite separable using cross polarization for the same reason, i.e.,

almonds have a higher DN value as compared to that of fallow/idle cropland and alfalfa (Table 22).

Cotton-fallow yields separability which is higher for like polarization as compared to cross polarization, where the TD values are both below 200. The overall separability of this class pair is below 1,700. It is surprising that like polarization (HH and VV) yielded higher TD values as compares to the VH polarization. The VH polarization had the most distinct DN values of 14 for cotton and 12 for fallow/idle cropland. Ideally the VH polarization would have resulted in the highest separability for cotton-fallow/idle cropland; however this was not the case.

Similarly, the class pair for cotton-alfalfa has extremely low separability across all bands primarily due to the similarity in DN values. Fallow/idle-alfalfa also follows a similar pattern where like polarization yields higher separability, as compared to cross polarization. The separability value for fallow/idle-alfalfa in the cross polarization would have been expected to be higher because the DN values are quite different from each other.

4.2.1.2 Radar Classification

Classification accuracies for the original radar data have been summarized in Tables 24, 25 and 26. The overall accuracies for all four individual bands range from 56% for the VH band (Table 25) to 73% for the HH bands (Table 24). The overall classification accuracy when all four radar bands (Table 26) are combined is 73%.

Table 24: Classification accuracies for individual radar bands (HH and HV), CA.

PALSAR HH					**Users Accuracy**
Land covers/uses	Almonds	Cotton	Fallow/Idle crops	Alfalfa	
Almonds	**19986**	4	156	3276	**85.3**
Cotton	3	**22993**	4737	374	**81.8**
Fallow/Idle Crops	1	1594	**2346**	470	**53.2**
Alfalfa	629	1109	5864	**4367**	**36.5**
Producers Accuracy	**96.9**	**89.5**	**17.9**	**51.5**	
Overall Accuracy					**73.2**
PALSAR HV					**Users Accuracy**
Land covers/uses	Almonds	Cotton	Fallow/Idle crops	Alfalfa	
Almonds	**20594**	0	37	21	**99.7**
Cotton	0	**14917**	7223	1190	**63.9**
Fallow/Idle Crops	0	9363	**4877**	2951	**28.4**
Alfalfa	25	1420	966	**4325**	**64.2**
Producers Accuracy	**99.9**	**58.0**	**37.2**	**51.0**	
Overall Accuracy					**65.8**

While the overall classification accuracies appear to be satisfactory, the producers accuracy for fallow/idle croplands and alfalfa are relatively poor.

Almonds, as expected, had excellent classification accuracies (above 90%) across all individual and the four stacked bands. These high classification accuracies for almonds can be validated by looking at the high DN values in Table 22. The DN values for almonds are quite high, as compared to other land covers/uses, making them highly separable from other classes.

Table 25: Classification accuracies for individual radar bands (VH and VV), CA.

PALSAR VV					**Users Accuracy**
Land covers/uses	Almonds	Cotton	Fallow/Idle crops	Alfalfa	
Almonds	**19590**	7	308	3035	85.4
Cotton	1	**20219**	2172	189	89.5
Fallow/Idle Crops	29	5149	**6450**	1577	48.8
Alfalfa	999	325	4173	**3686**	40.1
Producers Accuracy	**95.0**	**78.7**	**49.2**	**43.4**	
Overall Accuracy					**73.5**
PALSAR VH					**Users Accuracy**
Land covers/uses	Almonds	Cotton	Fallow/Idle crops	Alfalfa	
Almonds	**20605**	1	38	42	99.6
Cotton	0	**10350**	9854	1322	48.1
Fallow/Idle Crops	0	9677	**2766**	2498	18.5
Alfalfa	14	5672	445	**4625**	43.0
Producers Accuracy	**99.9**	**40.3**	**21.1**	**54.5**	
Overall Accuracy					**56.5**

Cotton was only accurately classified in the HH and VV bands, where the producers accuracy was above 78%. For all other individual and the four stacked bands the producers accuracy for cotton was quite poor. This poor classification of cotton relates back to the similarity in the DN values for cotton and fallow/idle. The majority of the misclassified pixels for cotton were fallow/idle cropland, hence emphasizing the importance of evaluating the similar DN values.

Fallow/idle cropland was also misclassified with other pixels - primarily cotton and alfalfa. The producers accuracy for fallow/idle cropland is extremely low across all bands, particularly the HH (20%) and VH (21%) bands. The producers accuracy for all

four bands was comparatively better than the individual bands, but it was still below the level of acceptability (70%).

Table 26: Classification accuracies for stacked radar bands (HH, HV, VH, VV), CA.

PALSAR HH, HV, VH, VV					**Users Accuracy**
Land covers/uses	Almonds	Cotton	Fallow/Idle crops	Alfalfa	
Almonds	**20616**	1	82	1737	91.9
Cotton	0	**16364**	3040	77	84.0
Fallow/Idle Crops	0	7788	**8778**	2495	46.1
Alfalfa	3	1547	1203	**4178**	60.3
Producers Accuracy	**100.0**	**63.7**	**67.0**	**49.2**	
Overall Accuracy					**73.5**

Alfalfa was also very poorly classified across all band combinations. The producers accuracy ranged from 43% to 54% for the individual bands, and only 49% when all four bands are stacked together. The majority of the misclassification for alfalfa was with fallow/idle cropland pixels. This was quite surprising, because the statistical values for the two classes are quite different.

Considering that three land covers/uses (cotton, fallow/idle cropland, and alfalfa) had exceptional low producers accuracy. The next step in the analysis focuses on evaluating the effectiveness of fusing multiple bands to increase those accuracies. This part of the analysis looks at the best two and three band combinations. These combinations of best bands are based on the overall classification of the individual bands.

Considering that the HH and VV bands yielded the best overall accuracies, they have been chosen for classification purposes. Similarly the HH, HV and VV bands have also been selected for the best three band combination (Table 27).

Table 27: Classification accuracies PALSAR scene. Best two and three band combination, CA

HH VV Best two bands					**Users Accuracy**
Land covers/uses	Almonds	Cotton	Fallow/Idle crops	Alfalfa	
Almonds	**20387**	4	198	3026	86.3
Cotton	0	**21419**	3060	160	86.9
Fallow/Idle Crops	0	2789	**5414**	1294	57.0
Alfalfa	232	1488	4431	**4007**	39.4
Producers Accuracy	98.9	83.3	41.3	47.2	
Overall Accuracy					**75.4**
HH, HV, VV best three bands					**Users Accuracy**
Land covers/uses	Almonds	Cotton	Fallow/Idle crops	Alfalfa	
Almonds	**20614**	0	80	1769	91.8
Cotton	0	**20294**	2987	108	86.8
Fallow/Idle Crops	0	4321	**8409**	2443	55.4
Alfalfa	5	1085	1627	**4167**	60.5
Producers Accuracy	100.0	79.0	64.2	49.1	
Overall Accuracy					**78.8**

The classification accuracies for the best two (Table 27) band combinations show marginal improvements over each band (HV and VH) taken individually. However, when a third band (HV) is added to the two band combination the overall accuracy increases to 79%, which is relatively higher than each band taken individually. The addition of an

extra band does validate the fact that adding bands increases the overall classification accuracies.

Unlike the Bangladesh study site, there are no distinct patterns which emerged during the analysis of classification accuracies for the individual radar bands. However, there is a relationship between the statistical DN values and producers classification accuracies for the four classes.

4.2.2 Radar Texture

This section highlights the separability values for the four different texture measures. As predicted the variance texture measure provided the best separability and was chosen for additional classification purposes.

4.2.2.1 Variance Texture

Table 28, shows the separability values for the radar image when variance texture is applied. The 13 x 13 window sizes yielded the best results as compared to the other three window sizes (5 x 5, 7 x 7, and 11 x 11).

The use of variance texture (13 x 13) is particularly helpful for class pairs which were inseparable using the original radar datasets. All class pairs showed improvement after texture was applied, except almonds-cotton and almonds-fallow/idle in the cross polarization. All bands which had opportunity for improvement, i.e., TD value of less than 2,000, did indeed yield higher separability after texture was applied.

Table 28: TD values for variance texture, CA.

Bands	Avg.	Min.	Almonds -cotton	Almonds-Fallow/idle	Almonds-Alfalfa	Cotton-Fallow	Cotton-Alfalfa	Fallow/idle-Alfalfa
TD values (5x5 Texture) for California, PALSAR image								
HH	894	51	61	1878	451	1721	51	1204
HV	1533	228	2000	2000	2000	1270	228	1700
VH	1587	155	2000	2000	2000	1542	155	1823
VV	917	0	0	1877	139	1943	92	1589
HH								
TD values (7x7 Texture) for California, PALSAR image								
HH	1041	0	0	1956	680	1893	282	1438
HV	1680	328	2000	2000	2000	1782	328	1969
VH	1685	224	2000	2000	2000	1895	224	1988
VV	1010	0	0	1953	222	1989	332	1757
TD values (11x11 Texture) for California, PALSAR image								
HH	1344	140	140	1994	1213	1979	1091	1648
HV	1766	598	2000	2000	2000	1996	598	2000
VH	1701	208	2000	2000	2000	1999	208	2000
VV	1261	188	188	1996	411	2000	1034	1935
TD values (13x13 Texture) for California, PALSAR image								
HH	1458	278	278	1998	1460	1988	1305	1720
HV	1745	469	2000	2000	2000	2000	469	2000
VH	1674	47	2000	2000	2000	2000	47	2000
VV	1352	312	312	1999	578	2000	1248	1972

Class pairs such as almonds-fallow/idle and cotton-fallow, which were inseparable using the original VV and HH bands, were now almost saturated with TD values of close to 2,000. Similarly, the cross polarizations (HV and VH) also shows improvements in the overall separability after texture is applied at a 13 x 13 window size. Class pairs for fallow/idle-alfalfa and cotton-fallow were inseparable in the original cross polarization (HV and VH), but after texture (13 x 13) is applied, both class pairs are highly separable with saturated TD values of 2,000.

Even though there is a major improvement in overall TD values after texture is applied there are still a few classes which are inseparable. In particular, it is the class pair for cotton-alfalfa which is inseparable across all bands with an average TD value of 312. Cross polarization for this class pair is relatively higher when compared to like polarization, however they are not high enough to provided adequate separability. In addition, the class pair for almonds-cotton has an average TD value of 156 for like polarization which makes them inseparable.

Variance texture was also calculated for the 5 x 5, 7 x 7, and 11 x 11 window sizes. There are certain patterns which emerge when multiple texture window sizes are used. As the window size increases, average TD values also increase. However, the TD value for VH starts to decrease as a larger window size is used as seen the Table 28.

The TD values for the 5 x 5 and 7 x 7 window sizes are better than the original TD values; however there are a few classes that have extremely low separability. The class pair for almonds-cotton has zero separability for the like polarization using the 7 x 7 texture window size. Similarly, the class pair of almond-alfalfa is also inseparable using like polarization in both texture window sizes. The class pair for cotton-alfalfa still remains inseparable across all bands for both texture window sizes.

Unlike the Bangladesh study site (7 x 7 window size), the best texture window size for this study site was 13 x 13. Even though there is an improvement in the overall separability values, there are still a few classes (cotton-alfalfa) which have poor separability across all bands after texture is calculated.

4.2.2.2 Skewness, Mean Euclidean Distance, Kurtosis

Table 29, summarizes the average TD values for the other three texture measures. Similar to the previous study area of Bangladesh, all field crops have minimum texture and hence are not separable. Cross polarization provides relatively better TD values, as compared to like polarization, however they are still quite low. None of these texture measures can provide good classification accuracies and hence are not considered for the next stage of analysis.

Table 29: TD values for the remaining Texture Measures, CA.

Bands	Avg.	Min.	Avg.	Min.	Avg.	Min.	Avg.	Min.
Skewness Texture Measure								
	5x5		7x7		11x11		13 x13	
HH	103	0	81	0	75	0	105	0
HV	355	56	368	72	365	0	354	0
VH	401	33	454	27	553	0	583	0
VV	144	0	148	0	146	0	176	0
Mean Euclidean Distance								
	5x5		7x7		11x11		13 x13	
HH	407	0	422	0	434	0	441	0
HV	858	91	893	97	943	97	963	98
VH	858	56	898	62	955	67	977	68
VV	360	0	376	0	393	0	399	0
Kurtosis								
	5x5		7x7		11x11		13 x13	
HH	0	0	1	0	30	0	61	0
HV	1	0	10	1	124	0	254	6
VH	2	0	8	1	83	0	172	0
VV	0	0	1	0	14	0	43	4

4.2.2.3 Radar Texture Classification

Variance texture measure yielded the best separability results, and hence it was selected for the next step of classification. In particular it was the 13 x 13 variance texture

that showed the most improvement over the original radar. Tables 30, 31, and 32 summarize the classification accuracies for the individual and multiple bands.

Similar to the classification results of Bangladesh, the use of texture did not help in improving the accuracies. Rather, there is a drop in the overall classification accuracies for most individual bands. The overall classification accuracy for the four bands (Table 32) dropped to 72% from an original 73%. Classification accuracies for certain classes such as alfalfa dropped drastically when texture is applied.

Table 30: Classification accuracies variance texture 13x13 (HH and HV), CA.

PALSAR HH					**Users Accuracy**
Land covers/uses	Almonds	Cotton	Fallow/Idle crops	Alfalfa	
Almonds	**19744**	20	165	3026	86.0
Cotton	0	**25552**	12611	160	66.7
Fallow/Idle Crops	0	0	**0**	1294	0.0
Alfalfa	875	128	327	**4007**	75.1
Producers Accuracy	**95.8**	**99.4**	**0.0**	**47.2**	
Overall Accuracy					**72.6**
PALSAR HV					**Users Accuracy**
Land covers/uses	Almonds	Cotton	Fallow/Idle crops	Alfalfa	
Almonds	**20618**	0	154	1	99.3
Cotton	0	**25699**	12808	7658	55.7
Fallow/Idle Crops	1	1	**46**	476	8.8
Alfalfa	0	0	95	**352**	78.7
Producers Accuracy	**100.0**	**100.0**	**0.4**	**4.1**	
Overall Accuracy					**68.8**

Cross polarization texture (HV and VH) were the only bands where the overall accuracies increase marginally as compared to the original radar dataset. The like

polarization (VV and HH), showed a reduction in their overall classification accuracies after texture is applied. Almonds and cotton classes for cross polarization show improvements in producers accuracy when texture is used. However the other two classes, fallow and alfalfa, both have reduced their producers accuracy. A similar pattern is evident in the like polarization where almonds and cotton result in an increased producers accuracy when texture is applied, however for the other two classes (fallow and alfalfa) the producers accuracy drops when texture is examined.

Table 31: Classification accuracies variance texture 7x7 (VH and VV), CA.

PALSAR VH					**Users Accuracy**
Land covers/uses	Almonds	Cotton	Fallow/Idle crops	Alfalfa	
Almonds	**20619**	0	168	1	99.2
Cotton	0	**25649**	12797	6211	57.4
Fallow/Idle Crops	0	48	**61**	1704	3.4
Alfalfa	0	3	77	**571**	87.7
Producers Accuracy	**100.0**	**99.8**	**0.5**	**6.7**	
Overall Accuracy					**69.1**
PALSAR VV					
Land covers/uses	Almonds	Cotton	Fallow/Idle crops	Alfalfa	
Almonds	**18867**	9	154	2332	88.3
Cotton	0	**25553**	11729	3382	62.8
Fallow/Idle Crops	0	89	**534**	580	44.4
Alfalfa	1752	49	686	**2193**	46.9
Producers Accuracy	**91.5**	**99.4**	**4.1**	**25.8**	
Overall Accuracy					**69.4**

Table 32: Classification accuracies for stacked variance texture bands, CA.

PALSAR Texture HH, HV, VH, VV					**Users Accuracy**
Land covers/uses	Almonds	Cotton	Fallow/Idle crops	Alfalfa	
Almonds	**20611**	0	160	675	**96.1**
Cotton	0	**25506**	12220	3892	**61.3**
Fallow/Idle Crops	2	27	**637**	1627	**27.8**
Alfalfa	6	167	86	**2293**	**89.9**
Producers Accuracy	**100.0**	**99.2**	**4.9**	**27.0**	
Overall Accuracy					**72.2**

Cotton and almonds were the two classes for which there is an increase in the producers accuracy when texture is applied to the original radar dataset. Overall cotton and alfalfa had good producers accuracy ranging from 90% to 100% for the individual bands and close to 100% accuracy when all four bands are stacked together.

The producers accuracy for fallow/idle croplands were exceptional low ranging from 0% to 4% for the individual band and 5% when all four bands are stacked. This is possible due to the edge pixels which have been misclassified after texture is applied to the radar image. The majority of the misclassification that occurred for fallow/idle cropland were with cotton. All pixels that should have been classified as fallow/idle cropland were misidentified as being cotton, resulting in low producers accuracy for the land cover/use.

Considering that two classes, fallow/idle cropland and alfalfa, still have low producers accuracy the next step focuses on fusing multiple bands to improve these accuracies. Table 33 summarizes the classification accuracies for the best two and three band combinations.

The overall classification for the best two and three band combinations is lower than when the bands are evaluated independently (original radar dataset). The overall classification for the best two (HH and VV) and three band (HH, HV and VV) combination dropped to 65% and 72% as compared to the original 75% and 79%. The drop in accuracies can be attributed to use of texture. Each of the individual texture bands yielded lower accuracies as compared to the original radar, and hence it is not surprising when these individuals texture bands are combined their accuracies are lower than the original radar dataset.

Table 33: Classification accuracies for best two and three band combination, CA.

HH, VV : Best two bands					**Users Accuracy**
Land covers/uses	Almonds	Cotton	Fallow/Idle crops	Alfalfa	
Almonds	**16280**	26	156	1691	**89.7**
Cotton	0	**25523**	11714	3256	**63.0**
Fallow/Idle Crops	2419	52	**55**	1153	**1.5**
Alfalfa	1920	99	1178	**2387**	**42.7**
Producers Accuracy	**79.0**	**99.3**	**0.4**	**28.1**	
Overall Accuracy					**65.2**
HH, HV, VV: Best three bands					**Users Accuracy**
Land covers/uses	Almonds	Cotton	Fallow/Idle crops	Alfalfa	
Almonds	**20614**	0	155	763	**95.7**
Cotton	0	**25625**	12142	3959	**61.4**
Fallow/Idle Crops	4	39	**708**	1928	**26.4**
Alfalfa	1	36	98	**1837**	**93.2**
Producers Accuracy	**100.0**	**99.7**	**5.4**	**21.6**	
Overall Accuracy					**71.8**

The patterns for overall and producers accuracy for the best two and three texture band combinations are very similar to those of texture bands taken individually. Almonds

and cotton provide good producers accuracy ranging from 79% to 100%. However, the two classes for fallow/idle cropland and alfalfa only yield producers accuracy ranging from 0.4% to 28%.

For classification purposes, radar texture did not yield any positive results but rather reduced the overall and producers accuracy for a few classes. This was surprising, considering that variance texture at a 13 x 13 window size, greatly improved the original TD value. It should have shown moderate improvements for classification. One of the reasons for this drop in classification accuracies might relate to the misclassification of the edge pixels. Similar misidentification of edge pixels (AOIs) was also noticed for the Bangladesh study areas, where the use of texture decreased the classification accuracies.

4.2.3 Radar fusion: Original Radar with Radar Texture

Table 34 summarizes the classification accuracies for original radar combined with radar variance texture.

Table 34: Stacked original radar with radar texture (variance7x7), CA.

HH , HV, VH, VV					**Users Accuracy**
Land covers/uses	Almonds	Cotton	Fallow	Alfalfa	
Almonds	**20619**	0	161	1562	**92.3**
Cotton	0	**19470**	4929	228	**79.1**
Fallow	0	5345	**7678**	2973	**48.0**
Alfalfa	0	885	335	**3724**	**75.3**
Producers Accuracy	**100.0**	**75.8**	**58.6**	**43.9**	
Overall Accuracy					**75.8**

A total of eight bands are evaluated to determine if the classification accuracies for alfalfa and fallow can be improved. Unfortunately, there is only a

marginal improvement in the overall classification accuracies. The overall accuracies increase to 76% from 73% (original radar) and 72% (variance texture).

Almonds and cotton both have good producers accuracies in the original and radar texture bands. Hence it is no surprise that when both datasets are fused the producers accuracies are quite good, i.e., 100% for almonds and 76% for cotton. There is a pattern that emerges when looking at producers accuracy for fallow/idle cropland and alfalfa. The producers accuracy for these two land covers/uses is based on the averages of the two datasets combined. The original radar yielded higher producers accuracy for fallow/idle (64%) and alfalfa (49%), however when these values are fused with radar texture the overall producers accuracy drops down to 59% for fallow/idle and 44% for alfalfa. One of the reasons for this is related to the low producers accuracy within the individual radar texture bands for fallow/idle and alfalfa.

The fusing of original radar datasets with radar variance texture did show minor improvements. However, there are certain classes such as fallow/idle cropland and alfalfa that have low classification accuracies (below 70%) regardless of the number and combinations of original and radar texture bands. Based on the assessment of the previous study area, these two land covers would have good accuracies using the optical dataset.

4.2.4 Landsat Thematic Mapper

The next focus of the study is to evaluate the statistical DN and separability values for the Landsat sensor. Similar to the original radar datasets, these DN values

provide validating information, which is useful when examining the separability and classification results. Table 35 contains the statistical values for spectral signatures extracted from the same AOIs using the TM image.

Table 35: AOI class statistic (DN values), TM image CA.

Land cover/use		**Bands**					
		Blue	**Green**	**Red**	**NIR**	**MIR**	**MIR**
Almonds	$\overline{X}$	87.16	44.98	48.20	109.16	101.12	48.39
	σ	12.64	9.69	16.87	16.41	25.38	21.57
Cotton	$\overline{X}$	99.20	50.39	60.25	58.16	103.58	61
	σ	3.97	3.08	4.34	4.54	10.54	7.74
Fallow/idle cropland	$\overline{X}$	107.95	58.49	72.87	71.81	129.82	79.19
	σ	10.31	6.75	9.53	10.12	19.03	13.30
Alfalfa	$\overline{X}$	85.39	39.42	38.51	124.28	96.93	39.64
	σ	8.61	5.90	10.77	30.74	11.24	11.06

Almonds have high DN values for the NIR and MIR bands, this is related to the reflectance properties of the IR bands. Both NIR and MIR bands are very responsive to chlorophyll level in the tree leaves. Considering the time of the year, almonds trees are fully emerged, and therefore have high reflectance in the NIR bands. The visible bands - blue (B), green (G) and red (R), have moderate DN values. The BGR have a shorter wavelength as compared to the infrared bands, hence they are more susceptible to scattering from the mid atmosphere.

Cotton has a relatively high DN value for the first MIR band. However, the DN values for the remaining bands are low. One of the reasons for the low DN values in all other band values might be because the cotton crop was not fully matured. Given the time

of the year (May) the cotton crop has not fully matured, hence resulting in low reflectance and DN values particularly in the NIR.

Fallow/idle croplands have DN values ranging from 58 to 107 for the visible bands and 71 to 129 for the infrared bands. Based on USDA metadata, this type of land cover/classification comprises of bare ground with leftover material after crops have been harvested. Considering that there is no healthy vegetation with high chlorophyll present on these fields, the DN values for the infrared bands should have been lower. However, this is not the case and the DN values for the infrared bands are the highest as compared to the other land covers/uses. This suggests that there is probably some type of grass/vegetation that is present on the ground.

Alfalfa as expected has high DN values for the first MIR bands. The first MIR band is most sensitive to green vegetation, and considering the time of the year, alfalfa is in full bloom and hence the high DN values for the first MIR bands. Similarly the NIR band also has high DN value for alfalfa.

4.2.4.1 Transformed Divergence

Table 36 summarizes the TD values extracted from the four AOIs. With the exception of almonds-alfalfa and cotton-fallow, most of the other class pairs are highly separable for all bands with TD values of well over 1,900.

Table 36: TD values for Landsat image, CA.

Bands	Avg.	Min	Almonds-Cotton	Almonds-Fallow/idle	Almonds-Alfalfa	Cotton-Fallow	Cotton-Alfalfa	Fallow/idle-Alfalfa
Blue	1631	685	2000	1999	1102	685	2000	2000
Green	1768	705	2000	2000	1901	705	2000	2000
Red	1806	850	2000	2000	1988	850	2000	2000
NIR	1419	0	1894	1997	664	0	1993	2000
MIR	1381	91	1998	2000	198	91	1999	2000
MIR	1664	176	2000	2000	1810	176	2000	2000

The class pair for almond-alfalfa is highly separable using the green, red, and second MIR bands. However in the blue and NIR channels, the separability ranges from only198 to 1,102. Considering the DN values for the two land covers/uses in the blue band are quite similar, this results in them having low separability. However, the DN values for the two cover types in the NIR and MIR channel are quite different. Almonds in the NIR band have a DN value of 109, where as the DN value for alfalfa in the NIR band is 124. Ideally this difference in the DN values should yield high separability, however this is not the case as seen in the separability values (Table 36).

Cotton-fallow/idle croplands have distinct DN values for all six bands, but the separability values are quite low. The separability values for this class pair ranges from 0 to176 in the infrared bands and 685 to 850 in the visible bands. In the previous section for radar classification, it was noticed that fallow/idle croplands were regularly misclassified as cotton. There appears to be pattern for these two cover types that makes them inseparable, resulting in poor classification accuracies (radar) and also low TD values as seen in Table 36.

4.2.4.2 Landsat Image Classification

All six Landsat bands were stacked together in order to evaluate the classification accuracies. Table 37 summarizes the classification accuracies for all four classes. The overall accuracy for the combined Landsat bands is 91%, which is a drastic improvement over the original radar (73%) and radar texture bands (72%). The stacking of Landsat bands is particularly useful for land covers which had extremely low producers accuracy in the radar bands.

Table 37: Classification accuracies for Landsat image, CA.

Blue, Green, Red, NIR, MIR, NIR					**Users Accuracy**
Land covers/uses	Almonds	Cotton	Fallow	Alfalfa	
Almonds	**16064**	0	484	241	95.7
Cotton	78	**24989**	322	0	98.4
Fallow	651	647	**12268**	3	90.4
Alfalfa	3826	64	29	**8243**	67.8
Producers Accuracy	**77.9**	**97.2**	**93.6**	**97.1**	
Overall Accuracy					**90.7**

Alfalfa and fallow/idle crops both have producers accuracy of well over 90%. This is vast improvement considering that alfalfa in the original radar dataset had an accuracy of only 49% and 27% when texture was applied. Similarly fallow/idle cropland has an accuracy of 67% in the original radar dataset and 4% when texture was applied. The producers accuracy for almonds dropped to 78%, as compared to the 100% in the original radar and radar texture bands. However, it is still well above 70%, and will be sufficient for classification purposes.

The classification accuracy results for California are quite similar to the previous study area of Bangladesh. Classes which have been consistently misclassified are now clearly distinguishable in the Landsat image.

4.2.5 Sensor Fusion

Based on the results of previous accuracies it is evident that the Landsat sensor is better suited for the land cover/use classification. Landsat imagery over the years has been an indispensible source of geographic information and its ability to accurately classify different land covers/uses makes it a good resource for scientific analysis. In past research (Huang et al. 2007) the fusing of radar with optical data has yielded higher land cover/use classification accuracies as compared to evaluating them individually. Even though the classification accuracies attained using Landsat images are quite good, the next step will evaluate if there are any improvements that can be made by fusing radar and optical data.

4.2.5.1 Layer stacking

The first dataset to be evaluated is the original radar layered stacked with Landsat. All four original radar bands (HH, HV, VH and VV) have been layer stacked with the six Landsat bands. The classification accuracies for both datasets stacked are summarized in Table 38. There is an increase in the overall classification accuracies (94%) when the two datasets are stacked, as compared to analyzing them independently.

Table 38: Classification accuracies for original radar and Landsat, CA.

All Ten Bands (Four radar and six optical)					**Users Accuracy**
Land covers/uses	Almonds	Cotton	Fallow	Alfalfa	
Almonds	**20619**	0	868	841	92.3
Cotton	0	**23638**	196	0	99.2
Fallow	0	1466	**11989**	9	89.0
Alfalfa	0	596	50	**7637**	92.2
Producers Accuracy	**100.0**	**92.0**	**91.5**	**90.0**	
Overall Accuracy					**94.1**

The producers accuracy for all four classes are excellent with all being over 90%, and only a few misclassifications for fallow/idle cropland and alfalfa. This is a vast improvement over the original radar datasets, where the two crops were regularly misclassified. The producers accuracy for alfalfa increased to 100% from 78% (Landsat). Similarly the users accuracy also increases to 92% from an original 68% (Landsat), when original radar and optical data are fused together.

The second data to be fused with Landsat is the radar variance texture (13 x 13). All four radar texture bands (HH, HV, VH and VV) have been layer stacked with the six Landsat bands. Table 39 summarizes the classification accuracies for the two datasets.

The overall classification accuracies are at 97%, which is an increase of almost 3% as compared to the previous combination of Landsat and original radar. Based on the overall classification accuracies of radar texture (72%) and radar (73%) it was expected that Landsat combined with original radar would have yielded higher accuracies, however this is not the case.

Table 39: Classification accuracies for radar texture (variance, 13x13) and Landsat, CA.

All Ten Bands (Four radar and six optical)					Users Accuracy
Land covers/uses	Almonds	Cotton	Fallow	Alfalfa	
Almonds	**20593**	0	228	383	**97.1**
Cotton	0	**25204**	664	0	**97.4**
Fallow	0	432	**12163**	10	**96.5**
Alfalfa	26	64	48	**8094**	**98.3**
Producers Accuracy					
	99.9	**98.1**	**92.8**	**95.4**	
Overall Accuracy					**97.3**

Similar to previous combinations of Landsat and original radar, all classes that had low producers accuracies are now above 90%. Once again there is little room for misclassified pixels as the accuracies for the land covers/uses are extremely high.

The combination of the Landsat data with radar and radar texture yields exceptionally good classification accuracies. These high accuracies can be directly attributed to the Landsat imagery. None of the radar datasets were able to successfully classify all land covers/uses independently, however when fused with the Landsat data the results were drastically improved. Fusing data from multiple sensors helps reduce any inconsistency during classification. For example, a band might have good producers accuracy in the Landsat data but very poor values in the radar texture; however, when the two sensors are fused an average is taken of both values. The resulting producers accuracy is more consistent and reliable, as compared to using either of the original datasets.

4.2.5.2 Principal Component Analysis (PCA)

PCA was done on the original four radar bands and then combined with the PCA of the six Landsat bands. The classification results of the original radar PCA and Landsat PCA are summarized in Table 40. Similar to the study area for Bangladesh, only two PCA bands were analyzed at a time, i.e., one component of radar and one component of Landsat.

The overall accuracy for this combination of PCA is 89%, which is comparatively lower than when both datasets are combined using a simple layer stacking procedure. As seen in Table 38, when the same datasets are combined using layer stacking the overall accuracy is 94%. More importantly this procedure of fusing data results in loss of key spectral information and is the reason for the low producers accuracy for alfalfa (57%).

Table 40: PCA of Landsat and original radar, CA.

First PCA of four radar and six Landsat bands					**Users Accuracy**
Land covers/uses	Almonds	Cotton	Fallow	Alfalfa	
Almonds	**20609**	0	60	1366	93.5
Cotton	0	**22042**	47	242	98.7
Fallow	0	871	**12986**	2032	81.7
Alfalfa	10	2787	10	**4847**	63.3
Producers Accuracy	**100.0**	**85.8**	**99.1**	**57.1**	
Overall Accuracy					**89.1**

The second combination of PCA involves the fusing of Landsat data with the radar variance textures (13 x 13). Table 41, summarizes the classification accuracies for the fused datasets. The overall classification for this dataset is 89%, which is lower than

the accuracies attained using traditional layer stacking for the same dataset i.e. Landsat and radar texture. Similar to the previous combination of PCA, there is loss of key spectral information, resulting in low producers accuracy for alfalfa (24%).

Table 41: PCA of Landsat and variance radar texture, CA.

PCA of four radar and six Landsat bands					**Users Accuracy**
Land covers/uses	Almonds	Cotton	Fallow	Alfalfa	
Almonds	**20619**	0	153	2	99.3
Cotton	0	**25325**	275	3719	86.4
Fallow	0	365	**12669**	2750	80.3
Alfalfa	10	10	6	**2016**	98.7
Producers Accuracy	**100.0**	**98.5**	**96.7**	**23.8**	
Overall Accuracy					**89.3**

During the execution of the PCA algorithm there appears to be loss of key spectral information, resulting in low producers accuracy. The overall classification accuracies for the PCA dataset (89%), is lower than both original datasets, i.e., original radar (91%) and Landsat (94%). However, in regards to fusing technique, layer stacking yielded better results as compared to PCA.

The overall patterns for classification accuracies for California were similar to Bangladesh. Radar yielded decent classification accuracies and separability values. The use of radar texture helped improve the overall separability among the land covers/uses. However, the use of texture for classification purposes did not prove beneficial. The classification accuracies were lower for the land covers/uses after texture was applied as compared to the original radar image. Landsat TM proved to be very useful in providing

good classification for all four classes. Fusing datasets from the two different sensors resulted in the highest classification accuracies for all classes.

4.3 Kenya

4.3.1 Original Radar

Prior to undertaking TD and classification analysis, statistics for the four AOIs have been extracted and presented in Table 42. These statistical values for the various land covers/uses have proved extremely valuable during the analysis of the previous two study sites, as they have helped establish patterns between separability values and classification accuracies.

Table 42: AOI class statistics (DN values) from the PALSAR scene. Mean and standard deviation, Kenya.

Land Cover/Use Classes	**Bands**				
		HH	**HV**	**VH**	**VV**
Residential	$\overline{X}$	24.58	12.10	12.14	21.71
	σ	11.89	4.65	4.67	10.29
Urban	$\overline{X}$	34.71	13.37	13.57	29.88
	σ	24.75	7.39	7.43	20.62
Savanna	$\overline{X}$	15.36	5.65	5.78	15.09
	σ	4.14	2.06	2.08	3.88
Bare ground	$\overline{X}$	10.91	4.09	4.18	10.89
	σ	4.16	1.59	1.61	3.82

The residential areas in this part of Kenya (Nairobi) have a high number of trees which are in close proximity to houses. This is one of the reasons for the high DN values ranging from 22 to 24 for cross polarization and 12 for like polarization. The presence of

houses along with trees strengthens the backscatter of the radar resulting in high DN values.

Urban areas identified in this study site are within Nairobi, and hence are heavily urbanized. These cultural features result in a high backscatter and high DN values. Similar to the residential class, cross polarization has lower DN values when compared to like polarization. This trend of cross polarization having lower DN values as compared to like polarization is common to all four classes.

Savannas in this part of the region are primarily comprised of shrubs and grass. The presence of small shrubs on the surface results in a high backscatter of the radar signal. Radar signals for savannas are strengthened because of the diversity of the ground features, which appear to have a rough texture.

Bare ground acts in a specular manner, reflecting energy away from the sensor. This is turn results in less energy backscattered to the sensor, causing the DN values to be comparatively low.

4.3.1.1 Transformed Divergence

The use of TD values in this study has been the foundation for evaluating the classification accuracies. Transformed divergence has not only helped select the optimum bands for classification, but has also provided a framework to better understand the various datasets. Table 43 summarizes the TD values for the radar datasets. The separability for all class pairs, with the exception of a few pairs, is satisfactory. There is room for improving these TD values by using texture measures.

Table 43: TD values for original PALSAR scene, Kenya.

Bands	Avg.	Min	Res-urban	Res-Savanna	Res-Bare	Urban-Savanna	Urban-Bare	Savanna-Bare
HH	1550	766	901	1645	1987	1999	2000	766
HV	1564	682	711	1990	2000	1999	2000	682
VH	1570	683	749	1987	2000	1999	2000	683
VV	1465	734	801	1323	1944	1990	2000	734

With the exception of residential-urban, savanna-bare ground, and residential-bare ground, all other class pairs have separability of over 1,950. The class pair for residential-urban has poor separability across all bands regardless of the type of polarization. These low separability values for residential-urban, relate to the similarity in their DN values. The TD values for like polarization would have been expected to be higher because the DN values are quite different. However, this is not the case and the class pair for residential-urban has poor separability.

Residential-savanna have excellent separability for cross polarization (1,990 and 1,987), but relatively lower separability in the like polarization (1,645 and 1,323). This variability in the TD values to some extent is unjustifiable, because the DN values for like polarizations are quite different, which would generally provide good separability.

Residential-bare ground have excellent separability across all bands. The high TD values for this class pair correlate directly to the unique DN values for each land cover/use. The DN value for residential and bare ground are very different from each other, hence resulting is good separability in all bands.

Similarly, the class pair for urban-savanna has excellent separability values. These high TD values are again reflected in the DN values for each of the two land covers/uses. The DN values for the two classes are very different from each other, which in turn results in achieving higher separability.

The class pair for urban-bare ground was able to achieve perfect separability with saturated TD values of 2,000 across all bands. This high separability was expected primarily because the backscatter from the urban areas is much higher as compared to that of bare ground.

Class pair savanna-bare ground is the least separable with extremely poor TD values across all bands. Theoretically this class pairs would be highly separable, however the DN values (Table 42) for the two cover types are similar to each other, resulting in low TD values.

4.3.1.2 Radar Classification

Classification accuracies for original radar have been summarized in Tables 44, 45 and 46. The best individual band was HH, with an overall classification accuracy of 71% (Table 44). When all four (HH, HV, VH and VV) are combined an overall accuracy of 77% (Table 46) is achieved.

Table 44: Classification accuracies for individual radar bands (HH and HV), Kenya.

PALSAR HH					**Users Accuracy**
Land covers/uses	Residential	Urban	Savanna	Bare ground	
Residential	**14983**	7354	11621	43	**44.1**
Urban	528	**10261**	2	6	**95.0**
Savanna	4041	377	**19334**	1793	**75.7**
Bare ground	29	2	1497	**21888**	**93.5**
Producers Accuracy	**76.5**	**57.0**	**59.6**	**92.2**	
Overall Accuracy					**70.9**
PALSAR HV					**Users Accuracy**
Land covers/uses	Residential	Urban	Savanna	Bare ground	
Residential	**17159**	14155	583	8	**53.8**
Urban	1636	**1756**	1078	7	**39.2**
Savanna	786	2076	**28330**	5180	**77.9**
Bare ground	0	7	2463	**18535**	**88.2**
Producers Accuracy	**87.6**	**9.8**	**87.3**	**78.1**	
Overall Accuracy					**70.2**

The residential class has producers accuracy ranging from 67% to 85% for the individual bands (Table 44 and 45) and 94% when all four radar bands (Table 46) are stacked together. Other than the 67% accuracy in the VH band, there were very few misclassifications. Understandably, the majority of the misclassified pixels for the residential class were with the urban class. This can be validated by looking at the DN values for VH, where residential and urban land covers have similar spectral signatures. Surprisingly the users accuracy for residential class was quite low. Similar to the misclassification of the producer accuracy, the majority of the misidentified pixels in the user accuracy were with urban.

Table 45: Classification accuracies for individual radar bands (VH and VV), Kenya.

PALSAR VH					Users Accuracy
Land covers/uses	Residential	Urban	Savanna	Bare ground	
Residential	**16377**	14473	1918	16	**50.0**
Urban	2412	**1672**	0	0	**40.9**
Savanna	792	1842	**28445**	7108	**74.5**
Bare ground	0	7	2091	**16606**	**88.8**
Producers Accuracy	**83.6**	**9.3**	**87.6**	**70.0**	
Overall Accuracy					**61.9**
PALSAR VV					**Users Accuracy**
Land covers/uses	Residential	Urban	Savanna	Bare ground	
Residential	**11465**	7699	15822	21	**32.8**
Urban	431	**9218**	119	4	**94.3**
Savanna	7461	1056	**15551**	1856	**93.7**
Bare ground	224	21	962	**21849**	**94.8**
Producers Accuracy	**58.6**	**51.2**	**47.9**	**92.1**	
Overall Accuracy					**84.7**

Urban land covers/uses had the worst producers accuracy, ranging from 10% to 57% for the individual bands and 64% when all four bands are stacked together. The majority of the misclassified urban pixels were assigned to the residential class. The HV band yielded the lowest producers accuracy of 10%. Similar to the previous class, the DN values for residential and urban in the HV band are very similar. This similarity in DN values relates to the low producers accuracy for the residential class.

The class for savanna had reasonable producers accuracy for all individual bands, ranging from 60% to 90%. When all four radar bands are stacked together the producers

accuracy drops to 63%. The majority of the misclassified pixels for savanna were residential.

Table 46: Classification accuracies for original radar bands, Kenya.

HH, HV, VH, VV					Users Accuracy
Land covers/uses	Residential	Urban	Savanna	Bare ground	
Residential	**18339**	6183	4483	44	**63.1**
Urban	603	**11489**	562	8	**90.7**
Savanna	536	160	**20345**	1633	**89.7**
Bare ground	103	162	7064	**22045**	**75.0**
Producers Accuracy	**93.7**	**63.8**	**62.7**	**92.9**	
Overall Accuracy					**77.0**

Bare ground as expected yielded the highest producers accuracy for the individual bands ranging form 70% to 92%. When all four radar bands are combined the producers accuracy stays at the 92% level. One reason that the high producers accuracy for bare ground is its low DN value making is highly separable from the other classes.

The best two and three band combinations (Table 47) also follow a similar pattern in their classification accuracies. The best two bands are comprised of like polarizations (HH and VV) yielding an overall accuracy of 69%. The overall accuracy of the best two band combinations is lower as compared to when both bands are evaluated independently. Urban and savanna both have low producers accuracy of 56%. However the producers accuracy for residential and bare ground is quite good (72% and 92%).

The best three band combination shows a moderate increase in the overall and producers accuracies. The overall accuracy when the third band (HV) is added increases to 77% as compared to the 69% for the best two band combination. Even though a third

band is added the producers accuracy for urban and savanna is below the level of acceptability (70%).

Table 47: Classification accuracies, best two and three band radar combinations, Kenya.

HH,VV Best two bands					**Users Accuracy**
Land covers/uses	Residential	Urban	Savanna	Bare ground	
Residential	**14208**	7316	10506	78	**44.3**
Urban	507	**10204**	49	4	**94.8**
Savanna	3463	311	**18427**	1678	**77.2**
Bare ground	1403	163	3472	**21970**	**81.3**
Producers Accuracy	**72.6**	**56.7**	**56.8**	**92.6**	
Overall Accuracy					**69.1**
HH, HV, VV Best three bands					**Users Accuracy**
Land covers/uses	Residential	Urban	Savanna	Bare ground	
Residential	**18391**	6158	4494	43	**63.2**
Urban	455	**11501**	457	8	**92.6**
Savanna	607	160	**20333**	1602	**89.6**
Bare ground	128	175	7170	**22077**	**74.7**
Producers Accuracy	**93.9**	**63.9**	**62.7**	**93.0**	
Overall Accuracy					**77.1**

Looking at the DN, TD, and classification values, it can be concluded that there is a direct relationship among the three. Classes which have similar DN values did not yield good TD or classification results. Classes which have distinct DN values provided higher separability and better classification results. The classification of radar data yielded satisfactory results; however, it would be beneficial to see if higher accuracies can be attained using texture measures on the original radar dataset.

4.3.2 Radar Texture

Following a similar pattern from the previous two study sites, variance texture measures provided the best separability results and hence was chosen for classification purposes. The other three texture measures were again unsuccessful in yielding any distinct separability values.

4.3.2.1 Variance

The 13 x 13 window sizes yields the best results as compared to the other three window sizes (5 x 5, 7 x 7 and 11 x 11). The TD results for all window sizes have been summarized in the Table 48.

Table 48: TD values for variance texture, Kenya.

Bands	Avg.	Min	Res-urban	Res-savanna	Res-Bare Ground	Urban-Savanna	Urban-Bare ground	Savanna-Bare ground
TD values (5x5 Texture) for Kenya, PALSAR image								
HH	1499	166	830	1998	2000	2000	2000	166
HV	1733	397	1999	2000	2000	2000	2000	397
VH	1736	414	1999	2000	2000	2000	2000	414
VV	1523	261	881	1994	2000	2000	2000	261
TD values (7x7 Texture) for Kenya, PALSAR image								
HH	1521	183	942	2000	2000	2000	2000	183
HV	1762	573	2000	2000	2000	2000	2000	573
VH	1764	587	2000	2000	2000	2000	2000	587
VV	1557	330	1011	2000	2000	2000	2000	330
TD values (11x11 Texture) for Kenya, PALSAR image								
HH	1547	210	1070	2000	2000	2000	2000	210
HV	1817	901	2000	2000	2000	2000	2000	901
VH	1813	879	2000	2000	2000	2000	2000	879
VV	1605	451	1179	2000	2000	2000	2000	451
TD values (13x13 Texture) for Kenya, PALSAR image								
HH	1559	235	1117	2000	2000	2000	2000	235
HV	1838	1029	2000	2000	2000	2000	2000	1029
VH	1833	999	2000	2000	2000	2000	2000	999
VV	1620	481	1241	2000	2000	2000	2000	481

The use of texture on radar images is particularly useful for the two class pairs of residential-urban and grassland-bare ground. These two class pairs had very poor separability in the original radar bands, however when texture is applied, there is a vast improvement in the TD values. The class pair for residential-urban had TD values of 711 and 749 for cross polarization in the original radar datasets. After texture is applied, the TD values for the same class pair are either saturated at 2,000 or are close to saturation. This increase in TD for the residential-urban class is common across all window sizes.

Similarly, the TD values for residential-savanna in the like polarization have shown drastic improvements. The TD value for residential-savanna in the original radar dataset were relatively low, however after texture is applied, the TD values are close to being saturated. It is these improvements in separability values for land covers/uses which make texture such a valuable tool.

For the third class pair (savanna-bare ground) which had the lowest separability in the original radar bands, there was only a marginal increase in TD values. While there are improvements in TD values for this class pair, the overall separability is below 1,700.

All window sizes helped increase the separability values for the classes. In particular it was the 13 x 13 window size that showed the most improvements over the original radar dataset. A larger window size was well suited for this study area, as it included a higher number of pixels, resulting in improved separability among the classes.

Overall there is an increase in TD values for most class pairs after variance texture is applied at multiple window sizes. However, there are still a few class pairs which have unsatisfactory separability values. The class pair for residential-urban was

highly separable in the cross polarization after texture was applied. However, the TD values for the same class pair in the like polarization were well below 1,700. Similarly the class pair savanna-bare ground is also inseparable.

4.3.2.2 Skewness, Mean Euclidean Distance, Kurtosis

Table 49 summarizes the TD values for the remaining texture measures in ERDAS. Unfortunately none of these texture measures are capable of providing useful separability results. It is rather disappointing to see that only one texture measure in the ERDAS module is capable of providing good TD values.

Table 49: TD values for the remaining texture measure, Kenya.

Bands	Avg.	Min	Avg.	Min	Avg.	Min	Avg.	Min
Skewness Texture Measure								
	5x5		7x7		11x11		13 x13	
HH	1334	20	1397	8	1409	0	1409	0
HV	1173	13	1378	13	1566	11	1610	
VH	1167	10	1374	10	1562	10	1606	10
VV	1332	41	1397	38	1411	21	1410	9
Mean Euclidean Distance								
	5x5		7x7		11x11		13 x13	
HH	1378	139	1414	136	1447	123	1454	113
HV	1238	104	1333	123	1421	140	1445	142
VH	1230	93	1326	108	1413	124	1437	126
VV	1322	152	1365	155	1409	147	1420	142
Kurtosis								
	5x5		7x7		11x11		13 x13	
HH	52	2	153	9	470	29	623	21
HV	66	0	0	0	0	0	0	0
VH	44	0	0	0	0	0	0	0
VV	56	0	174	0	0	0	753	17

The average separability for mean euclidean distance texture measures (Table 49) has been the highest among these three texture measures. Even though the average

separability was good, it was still not able to clearly distinguish the individual classes. For this reason none of these texture measures were selected for classification purposes.

4.3.2.3 Radar Texture Classification

The classification accuracies for variance texture at a 13 x 13 window size have been summarized in Tables 50, 51 and 52. In previous research studies (Huang et al, 2007; Idol et al. 2007), the use of larger window size yielded higher classification accuracies as compared to smaller window sizes. In this study site the classification accuracies for radar texture were quite variable. For some classes there is an increase in producers accuracy, however for others there is a drop. During the classification of the four land classes, the HV band did not yield good accuracy results for bare ground, and hence the results for this band have not been included.

During the classification of bare ground there were a few anomalies. Pixels in the HV band were misclassified as 0 and hence were interpreted as the background, resulting in voids/data gaps on the imagery. There is a misidentification of bare ground with savanna, however there were no data gaps, as opposed to cross polarization where the pixels were misclassified as the background resulting in data gaps. This was validated by looking at the radar image after texture was applied. The image for bare ground was extremely dark with pixel values of zero, hence it was no surprise during classification that all bare ground pixels in the HV band were classified as background. For verification purposes classification was also undertaken on the other window sizes, however the results were similar, i.e., the HV band was not able to successfully classify bare ground.

Table 50: Classification accuracies variance texture 13x13 (HH and HV), Kenya.

HH Radar Texture					**Users Accuracy**
Land covers/uses	Residential	Urban	Savanna	Bare ground	
Residential	**8714**	706	135	187	**89.4**
Urban	1976	**17113**	0	0	**89.6**
Savanna	378	0	**17134**	23007	**42.3**
Bare ground	8513	175	15185	**536**	**2.2**
Producers Accuracy	**44.5**	**95.1**	**52.8**	**2.3**	
Overall Accuracy					**46.4**
VV Radar texture					**Users Accuracy**
Land covers/uses	Residential	Urban	Savanna	Bare ground	
Residential	**6257**	1888	626	142	**70.2**
Urban	340	**15950**	0	0	**97.9**
Savanna	1854	0	**17206**	1032	**85.6**
Bare ground	11130	156	14622	**22556**	**46.5**
Producers Accuracy	**32.0**	**88.6**	**53.0**	**95.1**	
Overall Accuracy					**66.1**

Table 51: Classification accuracies variance texture 13x13 (VH), Kenya.

VH Radar texture					**Users Accuracy**
Land covers/uses	Residential	Urban	Savanna	Bare ground	
Residential	**18442**	15269	621	62	**53.6**
Urban	1110	**2722**	0	0	**71.0**
Savanna	0	0	**28702**	5639	**83.6**
Bare ground	29	3	2799	**149**	**5.0**
Producers Accuracy	**94.2**	**15.1**	**89.4**	**2.5**	
Overall Accuracy					**66.2**

As seen in Table 50, there is a drastic difference in the producers accuracy for bare ground. In the HH band the producers accuracy is much lower as compared to the

VV band. One of the reasons for this might be the orientation of the wavelength, i.e., VV is able to provide a stronger signal as opposed to using the HH band. Similarly a function of orientation also influences the producers accuracy for savanna and residential classes. Measuring both the amplitude and phase differences, the VH band is able to provide a higher producers accuracy for residential and savanna, as compared to like polarization where the accuracies are both below 70%.

These fluctuations in producers accuracy for individual bands are reflected in Table 52, when all bands are combined. Residential has a high producers accuracy based on the VH band, as opposed to the like polarization where the producers accuracies were very low. Urban has a high producers accuracy in all bands with the exception of the VH band, and hence it is no surprise when all bands are combined that the producers accuracy are also high. Savanna has a similar producers accuracy across all bands, resulting in a producers accuracy of 58% when all bands are combined. The only reason for bare ground to have a high producers accuracy when all bands are combined is related to the high accuracy (95%) in the VV band.

Table 52: Classification accuracies for stacked variance texture bands, Kenya.

HH, HV, VH and VV					**Users Accuracy**
Land covers/uses	Res	Urban	Savanna	Bare ground	
Residential	**18724**	2289	196	191	**87.5**
Urban	728	**15705**	0	0	**95.6**
Savanna	25	0	**18930**	1766	**91.4**
Bare ground	104	0	13328	**21773**	**61.8**
Producers Accuracy	**95.6**	**87.3**	**58.3**	**91.8**	
Overall Accuracy					**80.1**

The overall classification accuracy for the four radar texture bands is marginally better than the original radar dataset. The use of texture on the original radar data helped increase the accuracies from 77% to 80%. Even though there is an increase in the overall accuracies, the producers accuracy for savanna decreased to 58% from an original 63%. However, the remaining three land covers/uses all showed improvements in producers accuracy when texture was applied to the original radar dataset.

The majority of the misclassification for savanna was with bare ground. Pixels that should have been classified as savanna were misidentified as being bare ground, hence lowering the producers accuracy. Another interesting observation during the classification was the zero pixel values assigned to bare ground. The zero pixel values for bare ground were observed on all four window sizes.

4.3.3 Radar Fusion: Original Radar and Radar Texture

The effectiveness of fusing original radar with radar texture has been addressed in this section. Considering that there were a few anomalies in the dataset for radar texture, classification accuracies summarized in Table 53 are good and provide useful results. Interestingly, the producers accuracy for bare ground stays at the 90% level, similar to when both datasets are analyzed independently.

There is a marginal increase in the overall classification accuracies when the two datasets are combined. The overall accuracies increase to 83%, as compared to the 77% in the original radar data and 80% for radar variance texture. There is also an increase in the producers accuracy for all classes when the two datasets are combined. With the exception for savanna, all other classes have a producers accuracy of well over 70%.

Table 53: Stacked original radar with radar texture (variance13x13), Kenya.

HH, HV, VH and VV					Users Accuracy
Land covers/uses	Residential	Urban	Savanna	Bare ground	
Residential	**18910**	2814	671	178	**83.8**
Urban	603	**15180**	81	6	**95.7**
Savanna	47	0	**21705**	1714	**92.5**
Bare ground	21	0	9997	**21832**	**68.5**
Producers Accuracy	**96.6**	**84.4**	**66.9**	**92.0**	
Overall Accuracy					**82.8**

Savannas have a producers accuracy of only 67%. Once again there appears to be a misclassification of pixels. This misclassification for the savanna pixels was also seen in the original radar and radar texture. Pixels that should be classified as grassland are being misidentified as bare ground, lowering the producers accuracy for the cover type. This misclassification of pixels reverts back to the similarity in DN values for bare ground and savanna.

Overall the combined accuracy of fusing original radar with radar texture is quite good. However, there is still the one cover type, i.e., savanna which has low producer accuracy.

4.3.4 Landsat Thematic Mapper

The statistical DN and TD values for Landsat have been evaluated, and the results appear to provide useful information for the four classes. Table 54 summarizes the statistical data for Landsat.

Table 54: AOI class statistic (DN values), TM image, Kenya.

Land cover/use		**Bands**					
		Blue	**Green**	**Red**	**NIR**	**MIR**	**MIR**
Residential	$\overline{X}$	71.55	63.24	71.95	77.81	108.69	73.81
	σ	9.47	11.89	21.6	11.92	26.16	24.42
Urban	$\overline{X}$	97.81	89.88	107.84	71.10	125.70	103.72
	σ	14.28	14.80	19.77	12.62	23.75	22.46
Savanna	$\overline{X}$	85.01	78.67	102.74	78.89	152.74	100.97
	σ	4.54	5.98	11.08	6.11	12.25	10.26
Bare ground	$\overline{X}$	101.31	95.54	124.35	79.30	184.19	140.40
	σ	6.69	9.64	15.68	9.90	22.55	17.01

One of the drawbacks of the Landsat sensor is the similarity in spectral signature for residential and bare ground. The similarity in spectral signatures for these two land covers/uses is particularly true when there is substantial vegetation present in residential areas. However, as seen in Table 54, both classes are quite different in DN values and this would not be an impacting factor during classification. The DN values for all four land covers follow a similar pattern as seen in the previous two study sites. Never-the-less, it is crucial to uncover some of the underlying patterns in DN values to effectively evaluate a classified image.

Urban features have a high reflectance. This high reflectance is why there are high DN values across all bands. The DN values for urban range from 98 to 108 for the visible bands and 71 to 126 for the infrared bands. With the exception of the near infrared bands, there is a vast difference in DN values for urban and residential which would ideally make the two classes highly separable.

Savanna has high DN values for the infrared band. This can be attributed to the high reflectance from chlorophyll for the vegetated areas. The AOIs for savanna do include a few trees and this could also be increasing the overall DN values. The presence of chlorophyll on tree leaves is one of the primary reasons the DN values for this class are high. This has also been the case for the study area of Bangladesh, where the presence of trees resulted in high DN values.

Bare ground has the highest DN values for the four land covers. The values range from 95 to 124 for the visible bands and 70 to 184 for the infrared bands. Bare ground is relatively dry, almost acting like a mirror reflecting high amounts of energy back to the sensor.

4.3.4.1 Transformed Divergence

Overall the DN values for the four classes are quite unique, and hence the high separability among the classes. Table 55 summarizes the separability values for the six class pairs. As expected most of the class pairs are highly separable across all bands, with TD values of well over 1,700.

Table 55: TD values for Landsat image, Kenya.

Bands	Avg.	Min	Res-urban	Res-Savannah	Res-Bare Ground	Urban-Savannah	Urban-Bare ground	Grass-Bare ground
Blue	1908	1484	2000	1980	2000	1985	1484	1998
Green	1964	1812	2000	1998	2000	1976	1812	2000
Red	1888	1379	1992	2000	2000	1379	1961	1996
NIR	460	0	205	728	1093	1161	1802	0
MIR	1817	952	952	2000	2000	1954	2000	1996
MIR	1863	1400	1789	1989	2000	1400	1998	2000

With the exception of the NIR band, all other bands have good separability values. The only class pair for which NIR did provide good separability was for urban-bare ground with a TD value of 1,802. All other class pairs in the NIR band have TD values of less than 1,200, and in the case for savanna-bare ground there was zero separability. Overall the TD values for Landsat images provided good separability for most of the class pairs with the exception of the NIR band. The Landsat images were able to yield much higher separability values as compared to the original radar. The class pair of savannah-bare ground was inseparable with the radar dataset, however when using Landsat, the two cover types are quite separable with TD values close to 2,000. The only band in which this class pair did not yield good TD values was in the NIR band.

4.3.4.2 Landsat Image Classification

The classification accuracies for the Landsat image have been summarized in Table 56. The classification accuracies for Landsat in the two previous study sites have shown great improvements over the radar dataset. Hence it comes as no surprise for this study site that the classification accuracies for Landsat are superior to the original radar and radar texture band combinations.

Table 56: Classification accuracies for Landsat image, Kenya.

Blue, Green, Red, NIR, MIR and NIR bands					**Users Accuracy**
Land covers/uses	Residential	Urban	Savanna	Bare ground	
Residential	**17645**	2711	620	6	84.1
Urban	1904	**14902**	275	0	87.2
Savanna	32	302	**24124**	0	98.6
Bare ground	0	79	7435	**23724**	75.9
Producers Accuracy	**90.1**	**82.8**	**74.3**	**100.0**	
Overall Accuracy					**85.7**

The overall classification accuracies for the Landsat dataset is at 86%, and all producers accuracies are well over 70%. The classification accuracy for Landsat shows improvements over the original radar (77% overall accuracy), data by almost 8% and a 5% increase over radar variance texture (80% overall accuracy). The increase in overall accuracy results for Landsat is quite good, but more importantly is the increase in producers accuracy for savanna.

The land cover for savanna had a producers accuracy of below 70% in the original radar and radar texture bands. The majority of the misclassification for savanna in the radar bands was with bare ground. Pixels that should have been classified as savanna were misidentified as bare ground bringing the producers accuracy to 62% for original radar and 58% for radar texture. However, the same cover type in Landsat has a producers accuracy of 74% with comparatively less misclassified pixels.

Once again the use of Landsat images for classification has been a valuable addition to the analysis. Classes with low or unsatisfactory producers accuracies are now all above 70%.

4.2.5 Sensor Fusion

This section focuses on evaluating the classification accuracies for the three datasets. There are two procedures which are used to evaluate the classification accuracies. The first procedure is a simple layer stacking procedure followed by PCA analysis.

4.3.5.1 Layer stacking

The first multisensor dataset to be evaluated using layer stacking is for the original radar stacked with Landsat data. All four original radar bands were stacked with the six Landsat bands. Table 57 summarizes the results of this classification.

Table 57: Classification accuracies for original radar and Landsat, Kenya.

Land covers/uses	Residential	Urban	Savanna	Bare ground	**Users Accuracy**
Residential	**18854**	5169	1959	13	**72.5**
Urban	721	**12798**	232	2	**93.1**
Savanna	6	20	**20944**	1	**99.9**
Bare ground	0	7	9319	**23714**	**71.8**
Producers Accuracy	**96.3**	**71.1**	**64.5**	**99.9**	
Overall Accuracy					**81.4**

The overall accuracy of the combined datasets is 81%, which is a marginal increase when compared to the original radar dataset which had an overall accuracy of 80%. However, the overall accuracy for Landsat by itself was higher at 86%.Similarly the producers accuracies for all classes were also higher when Landsat data were classified independently. In particular, the producers accuracy for savanna decreased to 64% from an original 74% when Landsat data were analyzed independently.

The second dataset to be evaluated was for radar variance texture and Landsat. All four radar texture bands were layer stacked with the six Landsat bands (Table 58).

Table 58: Classification accuracies for radar texture (variance, 13x13) and Landsat, Kenya.

Land covers/uses	Residential	Urban	Savanna	Bare ground	**Users Accuracy**
Residential	**18450**	1731	115	130	**90.3**
Urban	1131	**16263**	0	0	**93.5**
Savanna	0	0	**21849**	11	**99.9**
Bare ground	0	0	10490	**23589**	**69.2**
Producers Accuracy	**94.2**	**90.4**	**67.3**	**99.4**	
Overall Accuracy					**85.5**

There are no vast improvements in classification accuracies by fusing the two datasets together. The producers accuracy for savanna is still below 70% and hence if selecting data for classification purposes it would be better to use Landsat by itself where the producers accuracy for savanna was 74%. Overall the original Landsat data had higher accuracies for all classes as compared to when it is combined with radar or radar texture.

4.3.5.2 Principal Component Analysis (PCA)

The following section evaluates the classification accuracies of the three datasets (original radar dataset, radar texture, and Landsat) by taking their first Principal Components. The principal component of all six Landsat bands were taken and combined with the first principal component of the original four radar bands (Table 59). Thereafter, the first principal component of all six Landsat was combined with the first principal component of four radar texture bands (Table 60).

Table 59: PCA of original radar and Landsat image, Kenya.

Land covers/uses	Residential	Urban	Savanna	Bare ground	**Users Accuracy**
Residential	**17378**	1813	21	0	90.5
Urban	1531	**15436**	5838	8	67.7
Savanna	391	184	**21192**	0	97.4
Bare ground	281	561	5403	**23722**	79.2
Producers Accuracy	**88.7**	**85.8**	**65.3**	**100.0**	
Overall Accuracy					**82.9**

The combination for both datasets i.e. PCA of Landsat with radar, and Landsat with radar texture, did not yield any improvements in overall classification. Similar to the results of layer stacking, the producers accuracy for savanna is lower when the two datasets (radar and Landsat) are combined. It is a better option to analyze the Landsat data by itself as opposed to fusing it with radar or radar texture.

Table 60: PCA of Landsat and variance radar texture, Kenya.

Land covers/uses	Residential	Urban	Savanna	Bare ground	**Users Accuracy**
Residential	**17529**	426	2285	0	86.6
Urban	1487	**17487**	130	120	91.0
Savanna	164	0	**21738**	0	99.3
Bare ground	401	81	8301	**23610**	72.9
Producers Accuracy	**89.5**	**97.2**	**67.0**	**99.5**	
Overall Accuracy					**85.7**

As seen in Table 59 the overall accuracy of Landsat and radar (83%) is lower than the original Landsat and radar taken independently. However, there is a marginal increase in overall accuracy when comparing the PCA results to the layer stacking

procedure. Even though the PCA accuracies are higher as compared to layer stacking, they are lower than the original datasets. A possible reason for the low accuracies attained using PCA might relate to the presence of noise on the radar data, and hence reducing the overall image quality (Roberts et al. 2008). The noise in this case was present in the radar data prior to undertaking any processing and this may have altered the PCA accuracies. It may be concluded that PCA and layer stacking of Landsat and radar data are not viable options for Kenya. The overall and producers accuracies are lower when both datasets are combined as opposed to when analyzing them individually. This is unlike the other two sites where layer stacking Landsat and radar yielded higher accuracies as compared to analyzing them individually.

5. Summary and Conclusion

Even though the findings in this study are limited to three sites, the results can be extended to other land cover/use studies. There are patterns which have been validated that can contribute to scientific research and knowledge in this area of geosciences. Considering that the use of radar imagery in the next few years will grow, it is important to assess and evaluate the functionality of this system individually and in combination with other traditional systems such as Landsat.

With an increase in the number of operational radar systems such as RADSARSAT-2 and TerraSAR-X, it is essential to gain a better understanding of some of the technological advancements in the application of remotely sensed data. In particular, it is the application of quad polarization radar data that remains in its nascent stages. It is only with a detailed understanding of this relatively new operational spaceborne quad polarization data that the scientific and application community can maximize the benefits of these technological innovations. This study has been able to provide some insight on the use of this technology for land cover/use classification. One of the major advantages of this research study is that the results are not based on any one particular study area, but rather encompassing three different regions across the world. Evaluating three study areas using the same methodology proved to be extremely valuable as it helped exclude discrepancies in the results and made it easier to compare

results across all three sites. Results for each of the three study areas have been summarized in the following sections.

Radar Datasets

All three study areas had average separability for the various classes in the original radar datasets. The separability for a few land covers/uses in all three study sites was quite low, i.e., below 1,500. These were classes which had similar DN values (spectral signatures) resulting in poor separability. Evaluating the DN values for all three study sites helped to get a better understanding for some of the patterns that existed. Without having a good understanding for the spectral signatures it would have been difficult to justify the low separability values for classes such as residential, forest, bare ground, and alfalfa to name a few.

The use of texture on all radar images proved to be an excellent procedure for increasing the separability among classes. Class pairs which were inseparable in the original radar dataset showed major improvements when texture was applied. In particular it was the variance texture measure that consistently provided the best separability for all three sites. The best texture window size for Bangladesh was 7 x 7, for California it was 13 x 13, and for Kenya is was also 13 x 13. Based on the results of this study, it can be concluded that a larger window size is better suited for land cover/use classification. Even though the 5 x 5, 7 x 7, 11 x 11 showed improvements in the separability values, it was 13 x 13 that provided the highest separability among the four classes for two of the three study areas.

Based on previous literature reviewed, it was predicted that texture would have an important role in improving the classification accuracies. Unfortunately, this was not the case and, surprisingly, the use of texture reduced the overall classification accuracies for Bangladesh and California. However, the use of texture for Kenya did show marginal improvements. Considering that two of three study areas were negatively affected by the use of texture, it was not a viable option for land cover/use classification. One of the reasons for texture yielding poor classification accuracies was related to the misclassification that occurred in the edge pixels of the AOIs after texture was applied.

When datasets for original radar and radar texture are combined for all three sites, there is a marginal increase in the classification accuracies. The increase in classification accuracies can be promising for future research. This may potentially be an important technique used by analysts who are only working with radar imagery and do not have optical data for classification purposes.

Landsat Datasets

Landsat images provided exceptionally good results for all three sites, yielding high separability and classification accuracies. In the cases of California and Kenya, Landsat images were able to provide higher separability for the classes as compared to the original radar and radar texture. However, for Bangladesh, the separability values from Landsat images were lower as compared to the original radar and radar texture. Based on the results of this study it can be concluded that Landsat images were able to provide higher separability for two of the three sites.

Classification accuracies attained using Landsat imagery were particularly helpful. Land covers/uses such as forest (Bangladesh), alfalfa and fallow/idle cropland (California) and savannas (Kenya) all had low producers accuracies (below 70%) for the original radar and radar texture combinations. The producers accuracies for all these classes were well above 70% using Landsat images.

The overall classification accuracies attained using Landsat images were superior to that of original radar and radar texture across all three study areas. Hence, based on the results of this study, it can be concluded that Landsat images were better suited for classification as compared to radar and radar texture.

Radar and Landsat

The question of whether classification accuracies can be increased by fusing multisensor data has been a key issue in the remote sensing community. The results based on the three areas identified in this study suggest that combining radar with optical data can indeed increase classification accuracies.

The study site for Bangladesh had excellent classification accuracies using Landsat images. Landsat images fused with original radar resulted in better classification accuracies as compared to when using radar texture. When comparing the two techniques, i.e., layer stacking and PCA, layer stacking was able to provided higher classification accuracies for the same datasets. California had similar results where fusing the multisensor data resulted in better classification accuracies (above 90%) as compared to taking either datasets individually. However, unlike Bangladesh, the combination of

Landsat and radar texture provided greater accuracies as opposed to original radar and Landsat. Using PCA as a fusing technique once again resulted in relatively lower classification accuracy as compared to layer stacking.

Unlike the other sites, the fusing of multisensor data for Kenya did not help increase the classification accuracies. The classification accuracies for Landsat evaluated independently were higher for all classes as compared to when it is combined with radar or radar texture. Hence for analysis purposes, it would be a better option to use the Landsat image by itself as opposed to fusing it with radar. The use of PCA for this study site resulted in marginal increases in classification accuracies compared to using layer stacking. Even though PCA provides slightly better classification accuracies, it is lower than the original Landsat and radar taken independently. Therefore, it is a better option to analyze the Landsat data by itself as opposed to fusing it with radar or radar texture.

Based on the results for these study sites it can be concluded that multisensor fusion is an excellent technique for increasing classification accuracies. Another advantage of fusing different datasets is the fact that it helps reduce any inconsistency during classification. For example, a band might have good producers accuracy for the Landsat data but very poor values for radar texture. However, when the two sensors are fused the resulting accuracies are more consistent and reliable as compared to using either of the original datasets.

It can also be suggested that layer stacking yields better classification accuracies as compared to PCA. During the execution of the PCA (algorithm) there appears to be loss of key spectral information which might be the reason for the relatively low

classification accuracies. One of the reasons for loss in key spectral information during PCA (algorithm) may relate to presence of speckle and noise in the original radar datasets.

The recent launches of multiple polarization spaceborne radar systems have made available to the geospatial industry a great wealth of data. Quad polarization radar data allows the scientific community to harness the potential of operational spaceborne radar data to assist projects in academia and private enterprise for planning, research and development purposes. The goal of this study was to explore the possibilities that this recently available quad polarization radar data offers and its effectiveness in classifying land cover/use in diverse regions around the world. The results from this study can potentially be extended to other sites to improve classification accuracies by fusing different sensor technologies.

Suggestions for Future Research

Having additional land cover/use classes could be beneficial for further research. Research oriented towards incorporating a higher number of complex land cover/use classes would be useful for uncovering some of the additional functionality of the quad polarization radar datasets. Secondly, evaluating the classification accuracies for larger texture window sizes would also be important.

Addition classification decision rules should also be investigated in order to compare the accuracies for the different procedures. Finally, evaluating different fusing

techniques such as Intensity Hue Saturation (IHS), Multiplicative Transform and Brovey Transform could also be examined in future research.

REFERENCES

REFERENCES

Anys, H., and. He, D., 1995. Evaluation of textural and multipolarization radar features for crop classification. *IEEE Transactions on Geoscience and Remote Sensing,* 33:1170-1181.

Banner, A. V., and Ahern, F. J., 1995. Incident angle effects on the interpretability of forest clearcuts using airborne C-HH SAR imagery. *Canadian Journal of Remote Sensing*, 2: 64-66.

Brisco, B., and Brown, R. J., 1999. Mulitdate SAR/TM synergism for crop classification in Western Canada. *Photogrammetric Engineering and Remote Sensing*, 61: 1009-1014.

Campbell, J.B., 2002. *Introduction to Remote Sensing* (New York, NY: Guilford).

Chavez, P.S., Sides, S.C., and Anderson, J.A., 1991. Comparison of three different methods to merge multiresolution and multispectral data: Landsat TM and SPOT Panchromatic. *Photogrammetric Engineering and Remote Sensing,* 57:295-303.

Center for Remote Imaging, Sensing and Processing (CRISP), National University of Singapore and SPOT Asia, Singapore (2001), http://www.crisp.nus.edu.sg/~research/tutorial/em.htm Accessed October 29 2008.

Dell'Acqua, F., Gamba, P., and Lisini, G., 2003. Improvements to urban area characterization using multitemporal and multiangle SAR images. *IEEE Transactions on Geoscience and Remote Sensing,* 41:1996-2004.

ERDAS Field Guide, 1999 (Atlanta, Georgia: ERDAS Inc.)

Gauthier, Y., Bernier, M., and Fortin, J. P., 1998. Aspect and incident angle sensitivity in ERS-1 SAR data. *International Journal of Remote Sensing*, 19:.2001-2006.

Haack, B.N., 2007. A comparison of land use/cover mapping with varied radar incident angles and seasons. *GIScience & Remote Sensing*, 44:1-15.

Haack, B.N., 1984. L and X-band like-and cross-polarized synthetic aperture radar for investigating urban environments. *Photogrammetric Engineering and Remote Sensing,* 50:331-340.

Haack, B. N., Solomon, E., Bechdol, M., and Herold, N., 2002. Radar and optical data comparison/integration for urban delineation: a case study. *Photogrammetric Engineering and Remote Sensing*, 68:1289-1296.

Herold, N., 2000. Integration of radar and optical data for land cover classification in the presence of speckle noise. Thesis, George Mason University, Fairfax, VA.

Hegarat-Mascle, S., Vidal-Madjar, D., Taconet, O. and Zribi, M., 1997. Application of shannon information theory to a comparison between L- and C-band SIR polarimetric data versus incident angle. *Remote Sensing of Environment,* 60: 121-130.

Henderson, F., Chasan, R., Portolese, J. and Hart Jr, J., 2002. Evaluation of SAR-optical imagery synthesis techniques in a complex coastal ecosystem. *Photogrammetric Engineering and Remote Sensing,* 68: 839-846.

Henebry, G.M. and Rieck, D.R., 1996. Applying principal component analysis to image time series: effects on scene segmentation and spatial structure. *IEEE Transaction on Geoscience and Remote Sensing.,*1:448-450.

Herold, N., Haack, B.N. and Solomon, E., 2005, Radar spatial considerations for land cover extraction. *International Journal of Remote Sensing,* 26:1383-1401.

Huang, H., Legarsky, J. and Othman J., 2007, Land-cover classification using Radarsat and Landsat imagery for St. Louis, Missouri. P*hotogrammetric Engineering and Remote Sensing*, 73:37-43.

Idol, T., B. Haack, S. Sawaya, and Sheoran, A., 2008. Land use/cover with quad polarization radar and derived texture measures, *Proceedings from American Society of Photogrammetry and Remote Sensing*, April 28 – May 2, 2008, Portland, Oregon (American Society for Photogrammetry and Remote Sensing, Bethesda, Maryland), unpaginated CD-ROM.

Islam, K.R. and Weil, R.R., 2000. Land use effects on soil quality in tropical forest ecosystem of Bangladesh. *Agriculture, Ecosystem and Environment*, 70: 9-16.

Jensen, J.R., 1996. *Introductory digital image processing: a remote sensing perspective,* second edition. Prentice Hall, Upper Saddle River, New Jersey.

Kurosu, T., Uratsuka, S., Maeno, H. and Kozo, T., 1999. Texture

statistics for classification of land use with multitemporal JERS-1 SAR single-look imagery. *IEEE Transactions on Geosciences and Remote Sensing,* 37: 227-235.

Latty, R. S. and Hoffer, R. M., 1980. Waveband evaluation of proposed Thematic Mapper in forest cover classification. *Proceedings of the Fall Technical Meeting, ACSM-ASP*, Niagara Falls, New York: RS-2-D-1 to RS-2-D-12.

Leckie, D.G., 1990. Synergism of synthetic aperture radar and visible/infrared data for forest type discrimination. *Photogrammetric Engineering and Remote Sensing,* 56:1237-1246.

Nikolakopoulos, K.G., 2008.Comparison of nine fusion techniques for very high resolution data. *Photogrammetric Engineering and Remote Sensing,* 74: 647-659.

Nyoungui, A., Tonye, E. and Alono, A., 2002. Evaluation of speckle filtering and texture analysis methods for land cover classification from SAR images. *International Journal of Remote Sensing,* 23:1895-1925.

Pal, S.K., Majumdar, T.J. and Bhattachrya, A.K., 2007. ERS-2 SAR and IRS-IC LISS III data fusion: A PCA approach to improve remote sensing based geological interpretation. *Journal of Photogrammetry and Remote Sensing*, 60: 281-297.

Puig, D. and Garci´a, M.A., 2001. Determining optimal window size for texture feature extraction methods. In IX Spanish Symposium on Pattern Recognition and Image Analysis, Castellon, Spain, 2:237–242.

United States Department of Agriculture (USDA), 2007. National agricultural statistics service, California cropland data layer (CDL).

Raghavswamy, V., Gautam, N.C., Padmavathi, M. and Badarinath, K.V., 1996. Studies on microwave remote sensing data in conjunction with optical data for land use/land cover mapping and assessment. *Geocarto International,* 11:25-30.

Roberts, J.W., Aardt, B.V. and Ahmed, F., 2008. Assessment of image fusion procedure using entropy and an image quality index. *International Journal of Remote Sensing.* In Review.

Saraf, A.K., 1999. IRS-IC-LISS-III and PAN data fusion: an approach to improve remote sensing based mapping techniques. *International Journal of Remote Sensing*, 20:1929-1934.

Schistad, A., Jain, A. and Taxt, T., 1994. Multisource classification of remotely sensed data: fusion of Landsat TM and SAR images. *IEEE Transactions on Geoscience and Remote Sensing*, 32:768-778.

Sheoran, A., Haack, B.N., Idol, T. and Sawaya, S., 2007. Land use/cover mapping comparison of optical and quad polarization radar imagery. *International Journal of Remote Sensing.* In review.

Simone, G., Farina, A., Morabito, F.C., Serpico, S.B. and Bruzzone, L., 2002. Image fusion techniques for remote sensing application. *Information Fusion*, 3:3-15.

Solber, A.H.S. and Anil, K.J., 1997. Texture fusion and feature selection applied to SAR imagery. *IEEE Transactions on Geosciences and Remote Sensing*, 10:989-1003.

Swain, P.H. and Davis (eds.), S.M., 1978. *Remote Sensing: the quantitative approach* (New York: McGraw-Hill).

Townsend, P.A., 2002. Estimating forest structure in wetlands using multitemporal SAR. *Remote Sensing of Environment,* 79:288-304.

Toyra, J., Pietroniro, A. and Martz, J., 2001. Multisensor hydrologic assessment of a freshwater wetland. *Remote Sensing of Environment,* 75:162-173.

Wen, C.Y. and Chen, J.K., 2004. Multi-resolution image fusion technique and its application to forensic science. *Forensic Science International,* 140:217-232.

Zhang, L., Zhao, Y., Huang, B. and Li, P., 2008. Texture feature fusion with neighborhood oscillating tabular search for high resolution image classification. *Photogrammetric Engineering and Remote Sensing*, 74:323-331.

CURRICULUM VITAE

Arjun Sheoran graduated from Carlisle School, Carlisle, Pennsylvania, in 2000. He received his Bachelor of Science from Shippensburg University of Pennsylvania in 2005. He was a Graduate Research Assistant in the Geography Department for two years and received his Master of Sciences in Geographic and Cartographic Sciences from George Mason University in 2009. He is currently working as a Geo Spatial analyst with Fugro EarthData in Frederick, MD.